Global and Planetary Change 220 (2023) 104011

Contents lists available at ScienceDirect

Global and Planetary Change

journal homepage: www.elsevier.com/locate/gloplacha

Fluid-rock interaction control on fault reactivation: A review of the Montmell-Vallès Fault System, central Catalan Coastal Ranges (NE Iberia)

Miquel Marín [a,b,*], Eduard Roca [b], Vinyet Baqués [c], Irene Cantarero [c], Lluís Cabrera [b], Oriol Ferrer [b], Anna Travé [c]

[a] SLB, Digital & Integration, Abingdon OX14 4RU, United Kingdom
[b] Institut de Recerca Geomodels, Departament de Dinàmica de la Terra i de l'Oceà, Facultat de Ciències de la Terra, Universitat de Barcelona (UB), Martí i Franqués s/n, 08028 Barcelona, Spain
[c] Institut de Recerca Geomodels, Departament de Mineralogia, Petrologia i Geologia Aplicada, Facultat de Ciències de la Terra, Universitat de Barcelona (UB), Martí i Franqués s/n, 08028 Barcelona, Spain

ARTICLE INFO

Editor: Zhengtang Guo

Keywords:
Poly-phase fault system
Structural inheritance
Fluid-fault rock interactions
Fault reactivation
Fault core
Fault rocks
Fault damage zones
Catalan Coastal Ranges

ABSTRACT

Structural inheritance is a key factor controlling the tectonic evolution of the central Catalan Coastal Ranges. Up to two periods of tectonic inversion (one positive during the Paleogene and the other negative during the Neogene) affected a previously well-developed Mesozoic extensional basin system and characterized the Cenozoic evolution of the area. In this scenario, tectonic fault inversion is often observed along the Montmell-Vallès Fault System. Fault reactivation shows differences along strike from NE to SW and appears decoupled from surface to depth due to its kinked-planar geometry and the change of fault dip from >60° to 30° in depth. The ability of the Mesozoic faults to be reactivated appears also influenced by changes in the mechanical properties of the inherited fault zone. Whereas the deeper and less dipping panels of the major faults are reactivated in the entire zone (contractional during the Paleogene and extensional during the late Oligocene-Neogene), the upper and highly dipping parts of the faults only show local reactivations. The observations indicate that fault dip, the indirect role of hosting lithologies (granites and siliciclastic metasediments versus carbonate rocks) on fault rocks, the indirect role of mineral precipitation and cementation product of fluid circulation, and the direct role of the mechanical properties of the resulting fault rocks (gouge versus cemented breccias) significantly control the fault reactivation. Upper crust low angle fault segments are easily reactivated during contractional deformation but not during the extensional one. Conversely, the segments with a high-angle dip are more easily reactivated during the extensional deformation but not during the contractional one. In the study area, this resulted in the formation of footwall short-cuts developed during the Paleogene compression and extensional short-cuts occurred during the Neogene extension. On the other hand, reactivation is effective in areas where granites and siliciclastic metasediments characterize the host-rock, and non-cohesive fault gouge forms the pre-existent fault core. Instead, fault reactivation appears restricted or even prevented where the host-rock includes thick carbonate successions, and the pre-existent damage zone is formed by highly cemented and cohesive breccias.

1. Introduction

Structural inheritance is widely accepted as a major structural control during the development of rift basins and orogenic belts. Pre-existing faults and basement heterogeneities constitute weakness zones that influence the location, the reactivation, and the amplification of later structures (i.e., during basin development or mountain building) (Jackson, 1980; Cooper et al., 1989; Buchanan and Buchanan, 1995; Butler et al., 2006; Butler, 2017; Torabi et al., 2019; Fossen, 2020; Lescoutre and Manatschal, 2020).

Tectonic inversion is observed in many basins and orogenic belts worldwide [i.e., the North Sea (Hansen et al., 2021; Scisciani et al., 2022), the Pyrenees (Buatier et al., 2012; Mencos et al., 2015), the Atlas (Teixell et al., 2003; Vergés et al., 2017) or the Andes (Perez et al., 2016; Ortiz et al., 2021)]. It is widely accepted that the geometry of the fault exerts a major control on its potential reactivation (Bond and McClay,

* Corresponding author at: Schlumberger, Digital & Integration, Abingdon OX14 4RU, United Kingdom.
E-mail address: mperez92@slb.com (M. Marín).

https://doi.org/10.1016/j.gloplacha.2022.104011
Received 13 June 2022; Received in revised form 24 November 2022; Accepted 2 December 2022
Available online 9 December 2022

1995; Ferrer et al., 2016; Roma et al., 2018). Other factors such as the relative orientation of the fault attitude to regional stresses (Amilibia et al., 2005; Bonini et al., 2012; Zwaan et al., 2022), fluid overpressures (Sibson, 2003; Peacock et al., 2016) or the mechanical strength of the inherited fault core (Wang et al., 1980; Wintsch et al., 1995; Bailey et al., 2005; Fossen, 2020) can also control fault reactivation. Among all these factors this work focuses on the impact of mineralizations and cementations on the mechanical properties of fault zones, a subject that is still poorly understood.

It is known that the type and characteristics of fault rocks control fault displacement-propagation ratios (Ferrill and Morris, 2008; Ferrill et al., 2011; Fossen, 2020). Likewise, the capacity of a fault to be reactivated is highly controlled by changes in the mechanical properties of the inherited fault zone, which essentially control the ability of the fault to be reactivated due to weakening or strengthening of fault rocks (Wang et al., 1980; Wintsch et al., 1995; Hausegger et al., 2010; Alder et al., 2016). The precipitation of cements and minerals within fault zones has frequently been described as a mechanism of increasing fault rock strength shifting the failure envelope to higher values (Wintsch et al., 1995).

The structure of fault zones has been the subject of research over the past decades. The role of cement precipitation in fault zones is an increasingly important factor recognized as modifying fluid flow conduits, strengthening faults, and providing evidence of fault history (Laubach et al., 2014). However, the extent of cement precipitation within a fault zone to control fault reactivation is still uncertain. Fluid flow through permeable or impermeable faults depends on its internal structure (e.g., fault rocks and/or precipitation of minerals) as well as on fault architecture and how the faults are arranged in three dimensions (Aydin et al., 1998; Agosta and Aydin, 2006). Most of the crustal-scale faults are organized into segments (Micklethwaite and Cox, 2004) and the growth, propagation, and interaction of these segments lead to the final architecture of the fault. The flow of fluids depends therefore on the connection status between fault segments in every stage of growth and the activity of the fault (Micklethwaite and Cox, 2004). The growth of a fault and the organization of segments in three dimensions are strongly controlled by horizontal discontinuities present in the stratigraphic record (Underwood et al., 2003; Soliva et al., 2005a, 2005b, 2006;

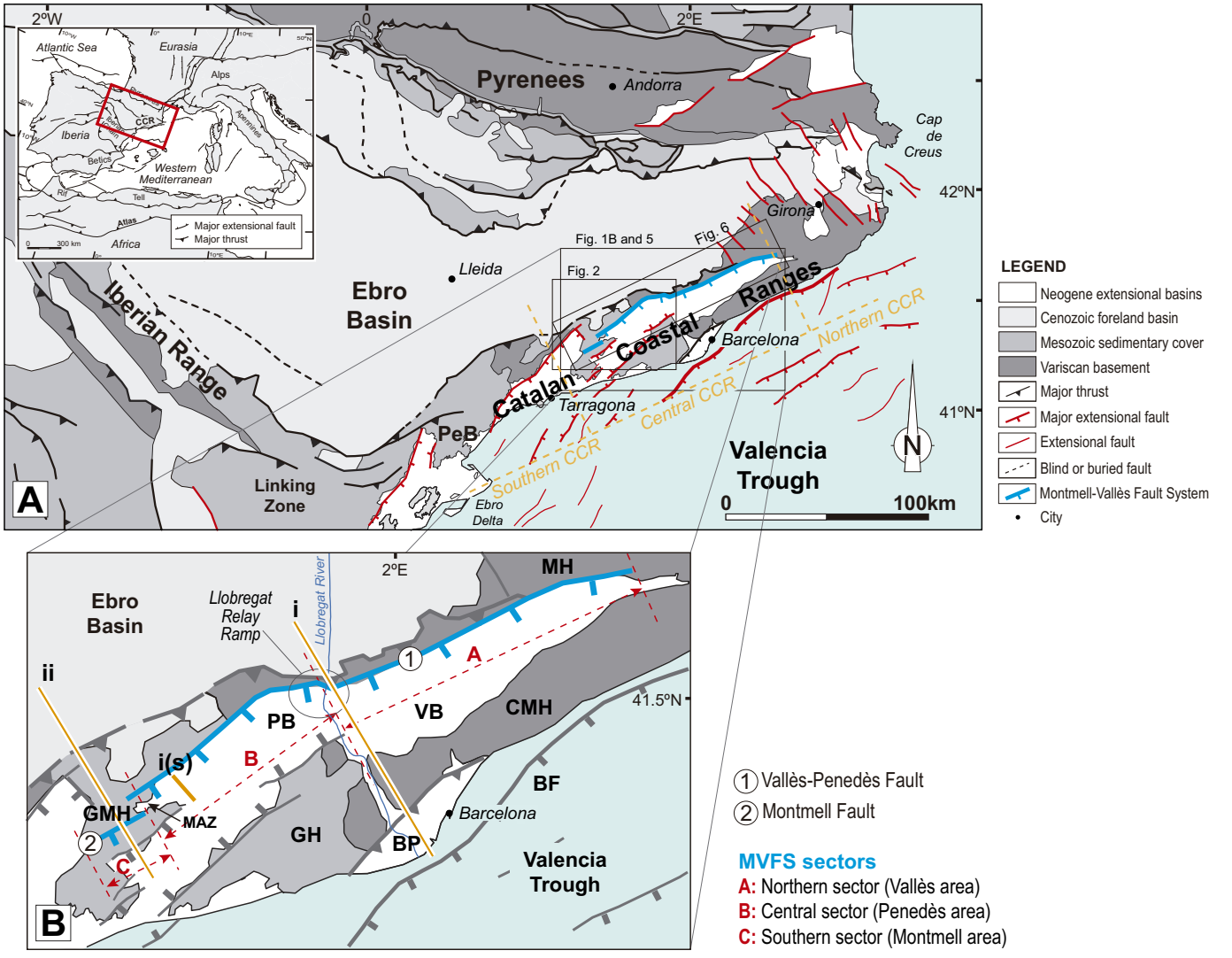

Fig. 1. A) Schematic geological map of NE Iberia showing the three major structural units bounding the Ebro Basin: the Pyrenees to the North, the Iberian Range to the SW, and the Catalan Coastal Ranges (CCR) to the SE. The trace of the Montmell-Vallès Fault System (MVFS) is highlighted with a thick blue line. The limits of the southern, central and northern domains of the CCR are indicated in orange (names and dashed-lines). Black squares indicate the location of Figs. 2, 5 and 6. The map in geographical coordinates. B) Detail of the central Catalan Coastal Ranges highlighting the three sectors of the Montmell-Vallès Fault System indicated in the text. The location of the structural sections and seismic profile shown in Fig. 3 is also indicated. **BF:** Barcelona Fault; **BP:** Barcelona Plain; **VP:** Vallès Basin; **PB:** Penedès Basin; **GH:** Garraf High; **GMH:** Gaià-Montmell High; **MH:** Montseny High; **CMH:** Collserola-Montnegre High; **PeB:** Perelló Basin; **MAZ:** Marmellar Accommodation Zone. (For interpretation of the references to colour in this figure legend, the reader is referred to the web version of this article.)

Micarelli and Benedicto, 2008). Often, fault segments are confined to specific layers of a given rheology and their interaction with neighboring segments depends on the ability of each segment to cross the bounding discontinuities of the layer (Naccio et al., 2005).

The presence of inherited faults is a key factor controlling the tectonic evolution of the Catalan Coastal Ranges (CCR) since Mesozoic time (Fontboté, 1954; Robles, 1982; Guimerà et al., 1995; Roca et al., 1999; Salas et al., 2001; Baqués et al., 2012; Marín et al., 2021). Some studies based on changes in regional stratigraphic thicknesses illustrate the control played by pre-Cenozoic structures (e.g., Esteban and Robles, 1976; Anadón et al., 1985; Guimerà and Álvaro, 1990; Salas and Casas, 1993; Gómez and Guimerà, 1999; Salas et al., 2001). Conversely, other studies based on geochemical investigations of fault rocks (i.e., fluid circulation and neoformation of minerals) disclose numerous reactivations since the Mesozoic (e.g., Baqués et al., 2014; Cantarero et al., 2014a) or even older (Marcén et al., 2018; Aldega et al., 2019).

During the last 25 years, several studies related to the influence of faulting processes on the distribution of diagenetic events during the evolution of the Catalan Coastal Ranges have been carried out. The main purposes of these studies have been a) characterizing from the petrological and geochemical point of view the minerals that fill the different fracture generations; b) determining the composition of the fluids that circulated through the different fractures; and c) establishing the paleohydrological regime for each of the main tectonic phases and determine the specific role of the fractures in each case. These studies have been mainly performed in four different areas (Figs. 1 and 2): 1) the Vallès half-graben (northern sector in Fig. 1B) where faults principally affect Paleozoic crystalline rocks (Bartrina et al., 1992; Cantarero et al., 2014a, 2014b, 2018), 2) the Penedès half-graben (central and southern sectors in Fig. 1B) where faults affect Mesozoic calcareous rocks and Miocene sandstone and evaporitic deposits (Calvet et al., 1996; Travé et al., 1998, 2009, 2021; Baqués et al., 2010, 2012, 2014; Moragas et al., 2013), 3) the Llobregat Transition Zone between the Vallès and Penedès half-grabens (Llobregat River, Fig. 2) in both Miocene rocks (Calvet et al., 2000, 2001; Travé and Calvet, 2001; Parcerisa, 2002; Parcerisa et al., 2005; Cantarero et al., 2014b) and basement granitoids (Serra and Enrique, 1989; Cardellach et al., 2002; Enrique and Solé, 2004), and 4) the Barcelona Plain, where the faults affect Paleozoic crystalline rocks and Triassic carbonate rocks (Santanach et al., 2011; Cantarero et al., 2014c) and the Miocene and Oligocene deposits (Gómez-Gras et al., 2000, 2001; Parcerisa, 2002; Cantarero et al., 2010, 2020).

In this paper, we integrate all these local works to provide a regional model and to unravel how diagenetic processes in the fault zone could have controlled reactivations experienced by the Montmell-Vallès Fault System in NE Spain (Figs. 1 and 2). In this regard, we present the characteristics of the fault zone during each of the main tectonic phases taking place in the area since Mesozoic times and their control on reactivation. The study provides a new regional basin model showing that fault reactivation is highly constrained by the lithology of the host-rock and the types of mineral precipitation within the fault zone, the lateral changes of which can be related with different degrees of tectonic inversion.

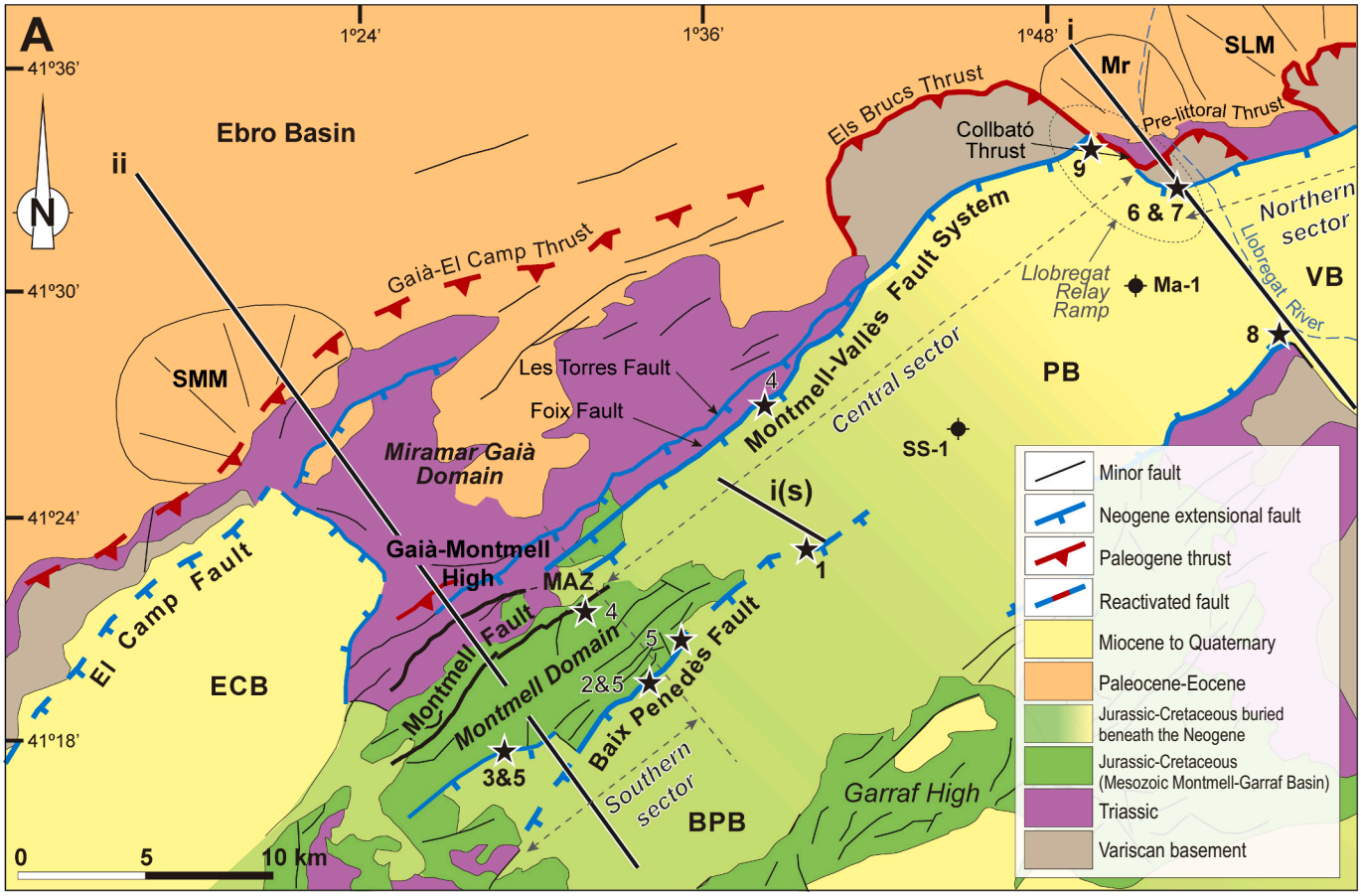

Fig. 2. Simplified geological map of the central Catalan Coastal Ranges highlighting the major Cenozoic faults and the sectors of the Montmell-Vallès Fault System indicated in the text. Star symbols indicate the location of fluid flow analysis in fault planes performed by (1) Travé et al., 1998, (2) Belaid et al., 2008, (3) Baqués et al., 2010, (4) Baqués et al., 2012, (5) Baqués et al., 2014, (6) Cantarero et al., 2014a, (7) Marcén et al. (2018), (8) Travé and Calvet (2001), (9) and Cantarero et al. (2014c). The location of the structural sections and the seismic profile shown in Fig. 3 is also indicated. **VB:** Vallès Basin; **PB:** Penedès Basin; **BPB:** Baix Penedès Basin; **ECB:** El Camp Basin; **MAZ:** Marmellar Accommodation Zone (Marín et al., 2021); **Ma-1:** Martorell-1 borehole; **SS-1:** San Sadurní-1 borehole. Paleogene alluvial and fan-delta systems: **SLM:** Sant Llorenç del Munt alluvial fan and fan delta; **Mr:** Montserrat fan delta; **SMM:** Sant Miquel del Montclar alluvial fan.

2. Geological setting

2.1. Tectonic framework

The Catalan Coastal Ranges (CCR) is a NE-SW-oriented structural unit in NE Iberia that extends parallel to the coastline for >250 km and has a basin-and-range configuration (Fig. 1). Nowadays, the CCR constitute the onshore part of the continental margin that separates the stretched crust of the Valencia Trough from the Iberian Plate (Roca and Guimerà, 1992; Dañobeitia et al., 1992; Vidal et al., 1995; Granado et al., 2016). This margin bounds the NW Mediterranean basin that resulted from the back-arc extension and rifting linked to the rollback of the Calabrian-Tethys subduction zone (Roca, 1994; Granado et al., 2016).

The current structure of the CCR is mainly controlled by the motion of 50 to 150 km-long ENE- to NE-trending faults involving the basement and displaying a right-stepping *en-echelon* outline. These major faults dip southeastwards and show normal, reverse, and/or restricted left-lateral strike-slip motion (Ashauer and Teichmüller, 1935; Llopis-Lladó, 1947; Anadón et al., 1985; Guimerà, 2004). They are detached on the base of the upper crust (Sàbat et al., 1997), and have associated fault propagation, fault bend and detachment folds developed in different Mesozoic to Cenozoic ages.

This structural configuration is the result of a complex evolution that comprises three main tectonic stages. The first stage, extensional, includes two rifting episodes that took place during the Permian-Early Triassic and the Late Jurassic-early Albian time spans. The older one was related to the early opening of the Neotethys, and the younger one resulted from the opening of the North Central Atlantic and the Bay of Biscay and the later uncoupling of the Iberian Plate from the Eurasian Plate (Srivastava et al., 1990; Salas and Casas, 1993; Salas et al., 2001; Sibuet et al., 2004; Gong et al., 2008). The second stage was contractional and spans from the Santonian to middle late Oligocene. It is related to the northward drift of Africa and the convergence and collision of the recently uncoupled Iberian and Eurasian plates (Srivastava et al., 1990; Rosenbaum et al., 2002; Angrand and Mouthereau, 2020; Romagny et al., 2020) that led to the formation of the Pyrenees (Muñoz, 1992; Vergés et al., 2002; Muñoz, 2017; García-Senz et al., 2019), the Iberian Chain (Guimerà, 1984; Guimerà et al., 1995; Nebot and Guimerà, 2016; Guimerà, 2018), and, in the present-day location of the CCR, the Catalan Intraplate Chain (CIC) (Anadón et al., 1985; Guimerà and Álvaro, 1990; Salas et al., 2001; López-Blanco, 2002). In the latter, the analysis of the preserved synorogenic Paleogene sequences denotes that the contractional deformation and uplift of the chain started in the Paleocene?-early Eocene at its NE end and progressed towards the SW up to the middle late Oligocene (Guimerà and Santanach, 1978; Guimerà, 1984; Anadón et al., 1985; Anadón, 1986; Barberà et al., 2001; Jones et al., 2004; Garcés et al., 2020). The third stage began in the latest Oligocene and has been active at least up the late Miocene (Bartrina et al., 1992; Roca et al., 1999). It is a new extensional phase linked to the subduction of the Tethyan Maghrebian Ocean beneath the Iberian Plate which induced back-arc processes and stretching in the eastern Iberian Plate from the rollback of the subducting plate (Horváth and Berckhemer, 1982; Fontboté et al., 1990; Roca and Guimerà, 1992; Roca, 1994; Carminati et al., 1998; Roca et al., 2004; Van Hinsbergen et al., 2014, 2020). This late Oligocene-Neogene extensional phase generated the present relief of the CCR from the extensional motion of crustal-scale SE-dipping extensional faults that compartmentalized the preexistent CIC into a series of NNW-tilted blocks (half-grabens and horsts) (Bartrina et al., 1992; Roca and Guimerà, 1992; Roca, 1994; Roca et al., 1999) and induced the isostatic uplift of their footwall blocks (Juez-Larré, 2003; Gaspar-Escribano et al., 2004).

In this polyphase tectonic scenario, it is widely accepted that fault reactivation became a major factor of control in the structural evolution of the CCR, at least, since Paleogene times. This control is clearly manifested in the extensional reactivation of Paleogene thrusts occurred during the Neogene extension (Fontboté, 1954; Anadón et al., 1979, 1985; Roca, 2001; López-Blanco, 2002; Gaspar-Escribano et al., 2004; Baqués et al., 2012; Marín et al., 2021); but also, by the recently observed inversion of some Late Jurassic-middle Albian rift-related extensional faults during the Paleogene compression (Salas et al., 2001; Baqués et al., 2012; Marín et al., 2021).

2.2. Stratigraphic framework

The CCR are made up by rocks that can be assembled into four different groups: 1) the Variscan basement made of pre-Cambrian and Paleozoic rocks, 2) the Triassic, Jurassic, and Cretaceous cover that unconformably overlies the Variscan basement and overprints mainly the southern half of the CCR, 3) the unconformably overlying Paleogene sediments of the Ebro Foreland Basin, and 4) the Miocene to Quaternary deposits filling and or onlapping the horsts and half-grabens.

The Variscan basement is formed by plutonic rocks (granites and granodiorites; Vaquer, 1973; Gil Ibarguchi and Julivert, 1988; Enrique, 1990; Enrique and Solé, 2004) intruding a thick metasedimentary succession composed of: 1) thick and predominant Pre-Cambrian and Cambrian-Ordovician fine-grained sandstones, limestones, acid tuffites, diabases and calcsilicate rocks; 2) Silurian black shales or slates with interbedded thin quartzite beds and sulfide layers; and locally preserved: 3) Upper Silurian to Devonian massive nodular limestones, nodular marlstones and varicoloured marlstones and shales; and 4) Carboniferous black cherts with phosphate nodules, carbonate/shale horizons and an overlying thick terrigenous sediments (Culm turbidite facies) (Durán and Julivert, 1990; Santanach et al., 2011).

The Mesozoic cover is integrated by Triassic, Jurassic, and Cretaceous *syn*-rift and/or post-rift sequences (Anadón et al., 1979, 1985; Salas et al., 2001). The Triassic is constituted by limestones, dolomites and locally siliciclastic and evaporitic rocks, ascribed to Buntsandstein, Muschelkalk and Keuper facies (Virgili, 1958; Calvet and Marzo, 1994; Arnal et al., 2002; Galán-Abellán et al., 2013; Escudero-Mozo et al., 2017; Ortí et al., 2017; Mercedes-Martín and Buatois, 2020). The Jurassic and Cretaceous succession is only preserved in the southern half of the CCR (Miramar-Gaià, Montmell and Garraf domains). It includes post-rift Lower-Middle Jurassic dolomitic breccias and dolostones, Upper Jurassic-Lower Cretaceous syn-rift limestones, dolostones and shale (Esteban and Julià, 1973; Salas, 1987; Salas et al., 2001; Albrich et al., 2006; Salas et al., 2020), and upper Albian to Cenomanian post-rift sandstones, mudstones, and carbonates (Anadón et al., 1979; Robles, 1982; Salas, 1987; Salas et al., 2001).

The Paleogene sediments of the Ebro Foreland Basin infill unconformably overlies the Mesozoic or even the Variscan basement. They consist of syn-contractional Paleocene to lower Oligocene marine and continental sediments (Ferrer, 1971; Anadón, 1978; Colombo, 1986; Garcés et al., 2020) that include large alluvial and fan delta systems at the toe of the CIC (SLM, Mr., SMM of Fig. 2). Inside the CIC, syn-contractional Upper Oligocene sediments are also locally present at the Barcelona Plain and northern edge of the Vallès-Penedès Basin. They consist of alluvial fan conglomerates, sandstones and muddy lacustrine sediments deposited in piggy-back or small pull-apart basins (Anadón et al., 1985; Roca et al., 1999; Parcerisa, 2002).

The CCR half-grabens formed during the late Oligocene-Neogene extension are filled by lower Miocene to Quaternary successions. In the central CCR, three depositional complexes have been identified in the Vallès-Penedès and Baix Penedès basins infill (Agustí et al., 1985; Cabrera and Calvet, 1996; Cabrera et al., 2004). The Aquitanian-upper Burdigalian Lower Continental Complexes made of thick alluvial fan red beds; the Transitional-Marine Complexes (late Burdigalian-early Langhian in age) encompassing coastal sabkha facies, carbonate coralgal platforms and siliciclastic alluvial fan-fan delta and bay facies; and the uppermost Langhian-Tortonian Upper Continental Complexes constituted by alluvial-fluvial and fluvial-deltaic red bed (Agustí et al., 1985; Cabrera et al., 2004). Over these syn-rift successions, there is a

deeply entrenched Messinian erosive surface, which also affected the older pre-Neogene rocks. This unconformity, in the incised valleys, is overlain by alluvial-fluvial (Gallart, 1981) and/or marine lower Pliocene to Quaternary units (Almera, 1894; Martinell, 1988; Corregidor et al., 1997).

3. Discussion

3.1. Mesozoic structure of the central Catalan Coastal Ranges

The structure of the CCR includes a set of Upper Jurassic-Lower Cretaceous extensional basins (Montmell-Garraf and Perelló basins, Figs. 1 and 2) the limits of which influenced on the location of major compressional structures during the Paleogene orogenic phase (Esteban and Robles, 1976; Anadón et al., 1979; Roca and Guimerà, 1992; Salas and Casas, 1993; Salas et al., 2001). These extensional basins essentially developed in the central and southern part of the CCR (e.g., Montmell-Garraf and Perelló basins, Fig. 1) while the northern part of the CCR remained as a structural high with no significant deposition during Upper Jurassic to Lower Cretaceous times at this area (Anadón et al., 1979).

The Cenozoic structure of the central CCR is mainly controlled by the major ENE-trending Barcelona, Vallès-Penedès and Montmell basement faults (Fig. 1). These faults dip to the SE and experienced Paleogene contractional and Neogene extensional motions (Bartrina et al., 1992; Roca and Guimerà, 1992; López-Blanco et al., 2000; Gaspar-Escribano et al., 2004; Marcén et al., 2018).

In the central part of the CCR, the northwestern boundary of the preserved Upper Jurassic-Lower Cretaceous successions filling the Montmell-Garraf Basin coincides with the trace of the Vallès-Penedès and Montmell faults (Fig. 2). These two faults include several branched segments and display a right-stepping *en-echelon* arrangement with a < 2 km trace separation (Figs. 1 and 2). Accordingly, they are treated as segments of the same fault system (here named Montmell-Vallès Fault System -MVFS-), the relay of which corresponds to the Marmellar Accommodation Zone described by Marín et al. (2021) (Fig. 2). The Mesozoic movement of this fault system is supported by the thickness variations of Upper Jurassic-Lower Cretaceous successions observed

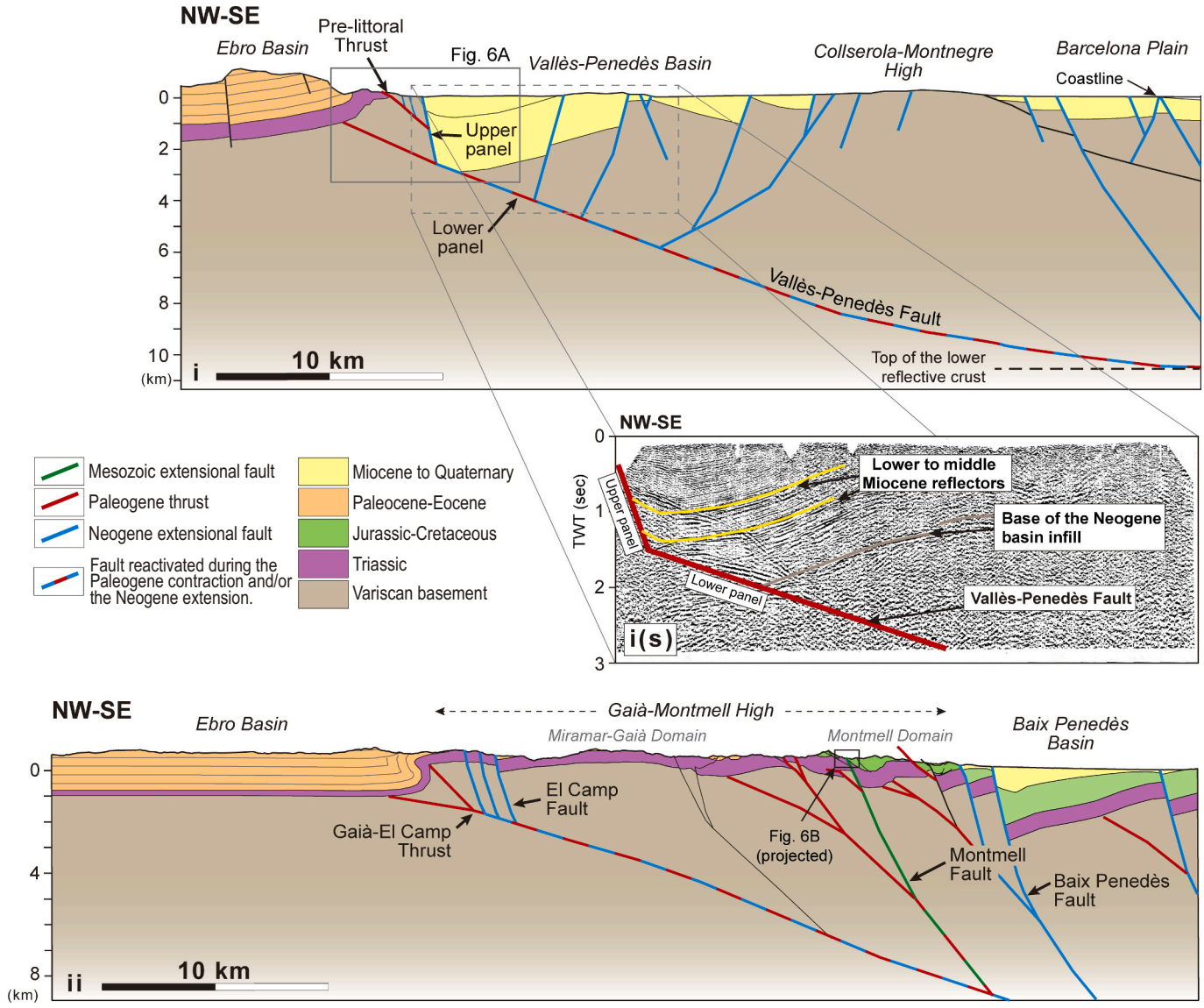

Fig. 3. Structural sections across the central Catalan Coastal Ranges: i: Llobregat section based on surface structural, fission track and Martorell-1 oil exploratory well data, i(*s*): PV-2 seismic profile with the interpretation of the Vallès-Penedès Fault with the base of the Vallès-Penedès basin infill and intrabasinal lower to middle Miocene reflectors (modified from Bartrina et al., 1992; see location in Fig. 1B); ii: Gaià-Montmell section (modified after Marín et al., 2021). See location of the sections in Fig. 2.

along its fault trace. Whereas in its footwall the Upper Jurassic-Lower Cretaceous is absent all along its fault trace, SW of the Llobregat River the hangingwall includes up to 1.2 km thick successions of this age (Fig. 3ii and 4A). The NW limit of the Upper Jurassic-Lower Cretaceous basin would therefore be assumed to correspond to the Penedès and Montmell segments of the MVFS (Fig. 4A).

Towards the NE, in the Llobregat River and Vallès area, the limits of the Montmell-Garraf Basin (Fig. 4A) are relatively uncertain due to the uplift and erosion of this sector of the CCR during the Paleogene contractional deformation. Nevertheless, they can be addressed from provenance analysis in the Paleogene terrigenous sediments of the SE margin of the Ebro Basin whose catchment areas were in the present-day CCR (López-Blanco et al., 2000). Thus, the composition of the clasts within the Sant Llorenç del Munt alluvial fan (SLM in the upper right

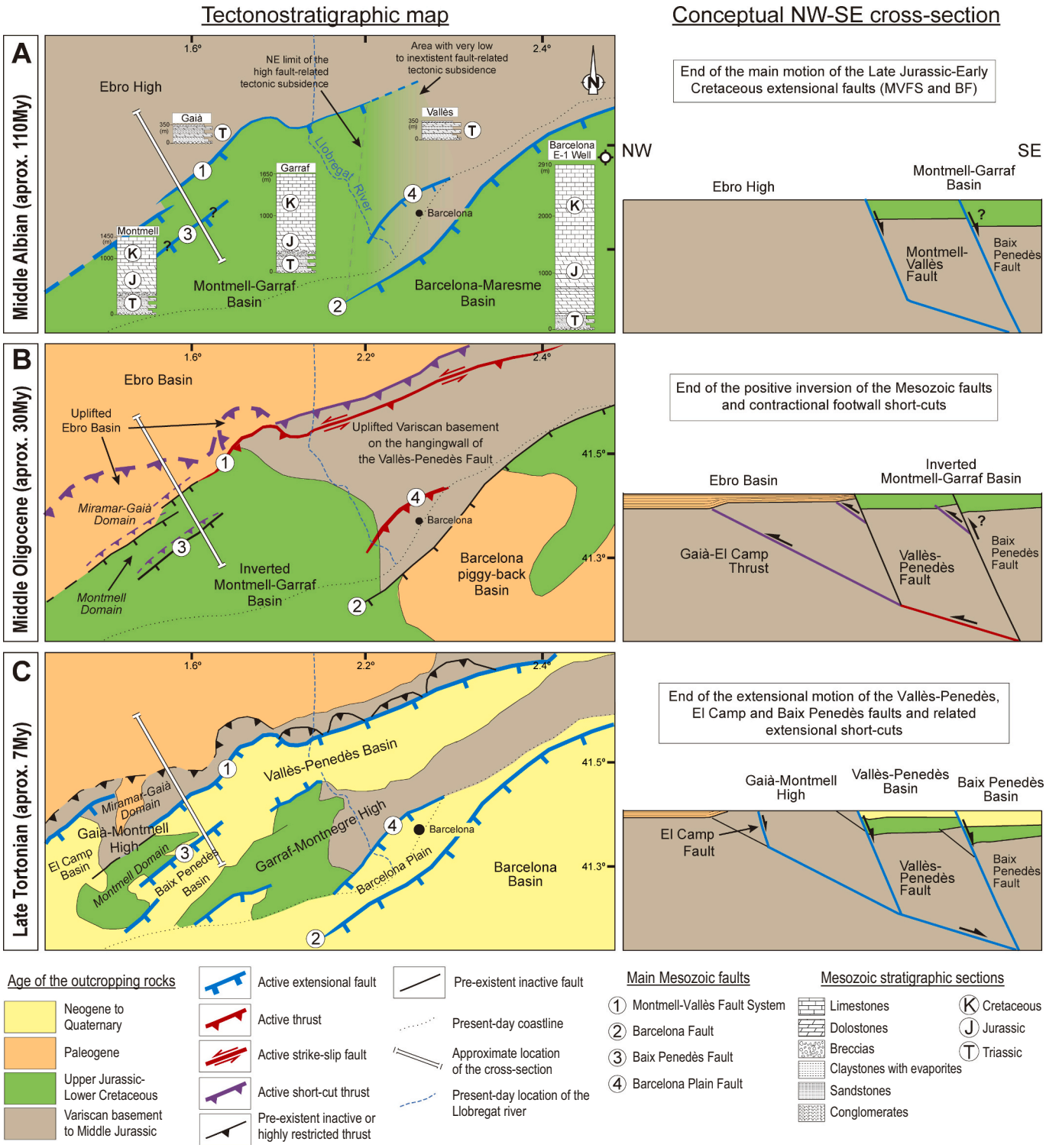

Fig. 4. Tectonostratigraphic maps and conceptual cross-sections showing the Late Jurassic (A) to late Miocene (C) evolution of the central Catalan Coastal Ranges. Map A includes sketched stratigraphic columns of the Mesozoic. On each map and cross-section active faults are shown with thick colored traces and lines, and previous inactive faults with thinner black lines.

corner of Fig. 2) denotes that, in the Vallès sector, the outcropping rocks in the eroded area were made by Triassic and Paleozoic rocks without or with a local and minor amount of Jurassic to Cretaceous rocks. Considering the lack of regional evidence of pre-Paleocene uplift and erosion of Jurassic and Cretaceous rocks, this would suggest that NE of the Llobregat River Jurassic and/or Cretaceous deposits were very thin or not present.

In contrast, syntectonic Paleogene detritical sediments in the Montserrat fan delta and the Sant Miquel del Montclar alluvial fan (Mr and SMM in Fig. 2) include frequent to predominant clasts deriving from the dismantling of Jurassic and mainly Lower Cretaceous successions (López-Blanco et al., 2000; Marín et al., 2021). This would indicate that SW from the Llobregat River, the catchment areas located SE of the MVFS and therefore the entire present-day CCR were made by Cretaceous rocks. Although, the current NE limit of the Jurassic and Cretaceous rocks preserved underneath the Neogene Vallès-Penedès basin infill is located approximately 10 km SW of the Llobregat River as sustained by the absence of rocks of this age in the Martorell-1 borehole and its presence in the San Sadurni-1 borehole (Lanaja, 1987; Bartrina et al., 1992) (Fig. 2 and stratigraphic sections in Fig. 4A), during the Upper Jurassic-Lower Cretaceous, the NE limit of the Montmell-Garraf Basin would be located close to present-day Llobregat River. The lack of Upper Jurassic-Lower Cretaceous successions NE of the Llobregat River denotes that during the Mesozoic the Vallès segment of the MVFS was inactive or had a minor displacement north of the Llobregat River (Figs. 4A and 5).

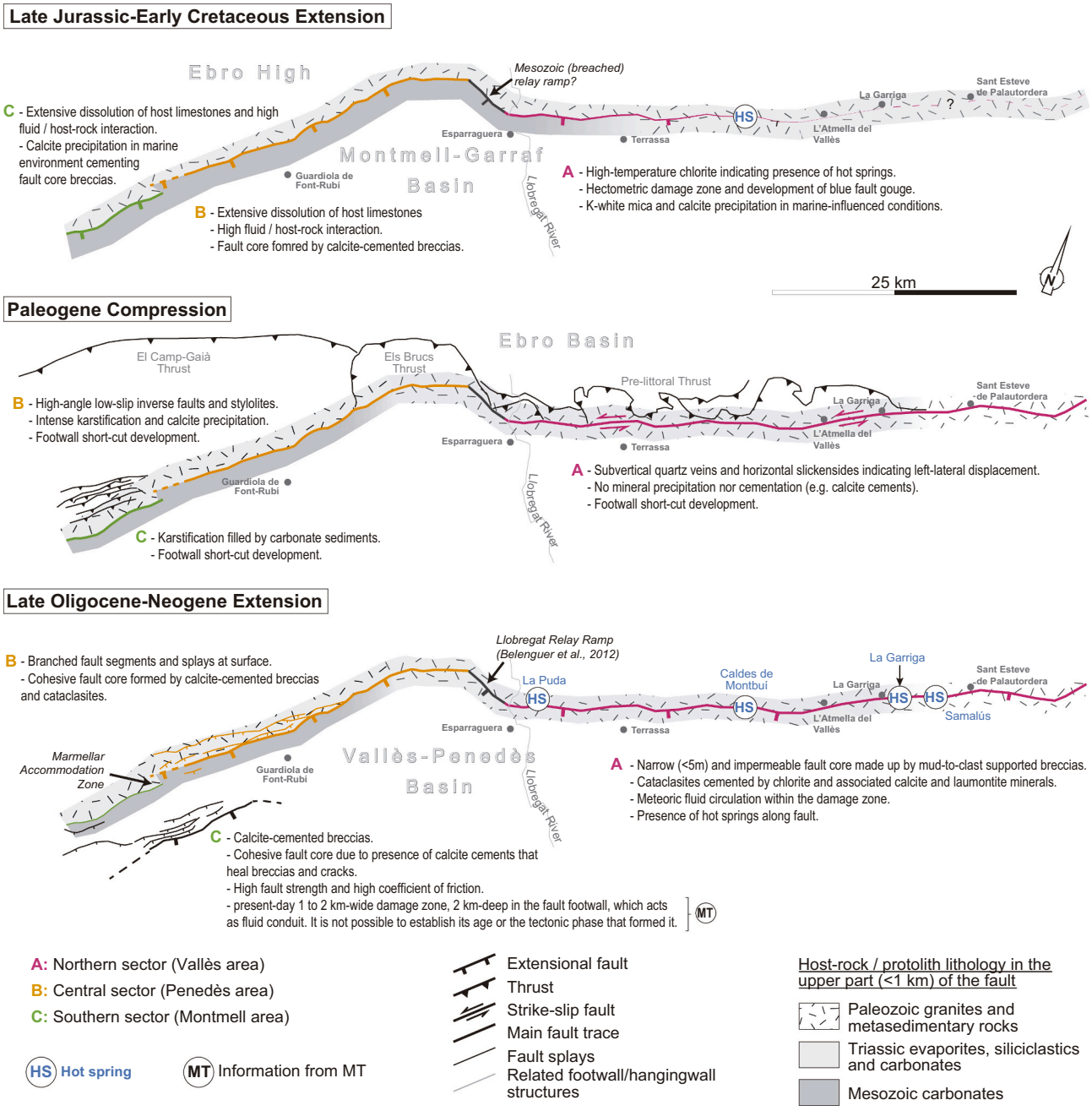

Fig. 5. Schematic map of the Montmell-Vallès Fault System showing fault damage zone characteristics of three sectors (A, B and C) during the different Late Jurassic-Early Cretaceous, Paleogene and late Oligocene-Neogene tectonic deformational stages. Fluid and petrological descriptions compiled after Travé and Calvet (2001), Baqués et al. (2008), Baqués et al. (2010), Baqués et al. (2012), Baqués et al. (2014) and Cantarero et al. (2014a, 2014c). Llobregat Relay Ramp from Belenguer et al. (2012). Magnetotelluric data (MT) from Marín et al. (2021).

The geometry of the Mesozoic active segments of the MVFS is poorly constrained with the available data. Only in some segments of the Montmell Fault where there is no Cenozoic reactivation, we can attest that, at surface, its plane was steeply dipping (>50°) towards the SSE (Fig. 3). At depth, the horizontal geometry of the highly reflective lower crust across the entire CCR (Sàbat et al., 1997; Vidal et al., 1998), which was formed at the end of the Variscan Orogeny (Bois, 1992), denotes that Mesozoic faults became nearly horizontal or slightly dipping towards the SE.

The Mesozoic structure of the central CCR appears also controlled by the parallel SE-dipping Barcelona Fault. This major Cenozoic fault, located offshore close to the present-day coastline (Fig. 1), has also been postulated as inherited from the Mesozoic and would correspond to the ancient NW limit of another Late Jurassic-Early Cretaceous extensional basin with >2 km thick infill (Roca and Guimerà, 1992; Roca et al., 1999; Gaspar-Escribano et al., 2004). The Mesozoic active Barcelona Fault and Montmell-Vallès Fault System display a right-stepped *en-echelon* configuration (Fig. 4A) and generated a WSW-dipping relay ramp in their overlapping area. This ramp, located at the present-day position of the Llobregat River, defined the NE limit of the Montmell-Garraf Basin, and was characterized by a thickness increase towards the WSW of the Upper Jurassic-Lower Cretaceous successions from 0 m to near 2 km.

3.2. Mesozoic structural inheritance in the central Catalan Coastal Ranges

The development of Paleogene basement involving ENE-trending folds and thrusts only in the footwall of the Montmell-Vallès Fault System (Figs. 2 and 3) indicates the partial positive inversion of the pre-existent Mesozoic MVFS during the Paleogene compressional phase (Gaspar-Escribano et al., 2004; Marín et al., 2021). Precisely, it evidences the thrust reactivation of the slightly dipping lower panel of the faults but not of the steep upper panels (Fig. 3). Here, the formation of footwall shortcuts indicates a practically not existent or negligible reactivation of the pre-existing fault planes as reverse faults. Due to their oblique orientation to the regional shortening direction (i.e., N-S shortening vs. NE-trending faults; Guimerà, 1984, 2004), these steep upper fault panels show instead reactivation as left-lateral strike-slip faults (Anadón et al., 1985). Nevertheless, such transpressional reactivation is not general. It has been observed in the Vallès area of the MVFS (Julià and Santanach, 1984, 1998) but not in the southwestern part of this fault system. Here, at surface, the Mesozoic Montmell Fault does not show any kind of Paleogene contractional reactivation but the development of buttressing structures (minor folds, thrusts and backthrusts) in their hangingwall (Figs. 4B and 6B).

In relation to the areal distribution of the interpreted footwall shortcuts, the presence of this kind of structures in the Vallès segment of the MVFS suggests that the Mesozoic fault bounding the Upper Jurassic-

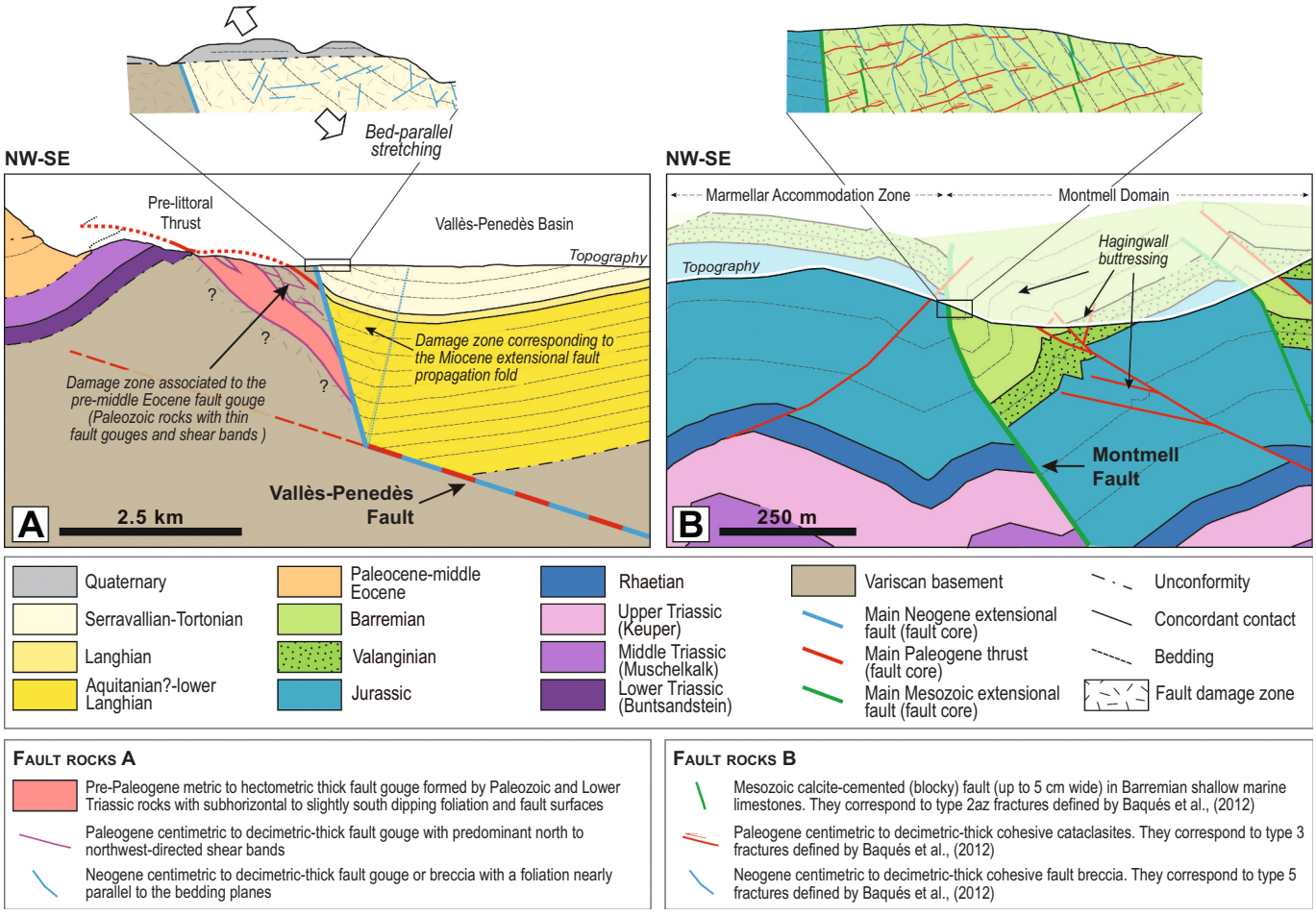

Fig. 6. A: Geological section of the Vallès-Penedès Fault in the northern sector of the Montmell Vallès Fault System showing the characteristics of the fault zone. Zoomed area: sketch of the Colònia Sedó outcrop highlighting Neogene fractures related to the hangingwall damage zone. B: Geological section across the Montmell Fault in the Marmellar Accommodation Zone area in the southern sector of the Montmell Vallès Fault System (modified from Marín et al., 2021). Zoomed area: sketch of the Riera de Marmellar outcrop highlighting Mesozoic, Paleogene and Neogene fractures related to the hangingwall damage zone (modified from Baqués et al., 2012). Fracture types are not to scale. A & B sections located in Fig. 3.

Lower Cretaceous Montmell-Garraf Basin extended further to NE than the defined basin infill limits, at least up the present-day location of the La Garriga town (Fig. 5).

Later during the late Oligocene-Miocene extensional stage, the inherited MVFS was also reactivated. The low-dipping lower fault panels moved again in an extensional sense (Gaspar-Escribano et al., 2004) whereas the steep upper ones show a broad partial reactivation, in this case as extensional faults. The reactivation of the steep upper panels is restricted to the northern and central sectors of the MVFS (Vallès and Penedès areas) where the outcropping Vallès-Penedès Fault follows the trace of the Mesozoic fault at the regional scale. However, the Neogene fault does not always reactivate the preexistent Mesozoic fault core but developed close in their hangingwall (Fig. 5) as extensional shortcuts of the preexistent thrusts (Fontboté, 1954; Anadón et al., 1985; Roca and Guimerà, 1992). In contrast, the steep upper panels of the southern sector of the MVFS (Montmell area), once again, remained inactive during the Neogene extension. Here, the extensional reactivation of the low-angle lower fault panel resulted in the formation of an extensional shortcut represented by the Baix Penedès Fault (Marín et al., 2021) (Fig. 3ii and 4C).

Summarizing, the MVFS shows reactivation during the Cenozoic, first under contraction during the Paleogene (Juez-Larré and Andriessen, 2006; Marín et al., 2021) (Fig. 4B), and later under extension during the late Oligocene-Neogene (Fontboté, 1954; Anadón et al., 1985; Roca and Guimerà, 1992; López-Blanco et al., 2000) (Fig. 4C). Nevertheless, such reactivation is not complete. The upper steep panels of the inherited Late Jurassic-Early Cretaceous faults only reactivated partially in the northeastern sectors of the MVFS but not in its southwestern ones.

3.3. *Differences in the fault zone deformation of the steep upper fault panels along the Montmell-Vallès Fault System*

Up to three sectors with different Mesozoic and Cenozoic fault zone deformation are distinguished along the steep upper fault panels of MVFS: 1) a northern sector that corresponds to the Vallès area (Fig. 2) and extends from the Llobregat Relay Ramp to the ENE fault system edge located SE of the Montseny High (see location in Fig. 1); 2) a central sector extending along the Penedès area SW from the Llobregat Relay Ramp to the Marmellar Accommodation Zone (Figs. 1, 2 and 5); and 3) a southern sector that corresponds to the Montmell area and includes the Montmell and Baix Penedès faults (Figs. 2 and 5).

3.3.1. *Northern sector (Vallès area)*

This sector of the MVFS developed over a host-rock or protolith mostly formed by granitoids and metasedimentary siliciclastic rocks of the Variscan basement and, at superficial levels, by thin Triassic carbonate and siliciclastic rocks and thicker Cenozoic *syn*-kinematic siliciclastic sediments (sector A in Fig. 5). The geometric, deformational, and petrological characteristics of the northern sector of the MVFS are summarized in the Table 1.

This sector includes three different fault zones linked to the three stages of the MVFS evolution: a) a first subvertical fault zone restricted to the footwall of the Paleogene Pre-littoral Thrust; b) a second fault zone slightly dipping to the SE that follows this Paleogene thrust; and c) a third fault zone linked to the late Oligocene-Neogene extension of the Vallès-Penedès Fault. The first one is formed by a vertical to very steep SSE-dipping fault zone with a width ranging from some hundreds of meters to a kilometer (Anadón et al., 1985; Julià and Santanach, 1984,

Table 1
Characteristics of the northern sector (Vallès area) of the Montmell-Vallès Fault System. Compiled from Anadón et al. (1985), Julià and Santanach (1984, 1998), Camps and Morera (2014) and Cantarero et al. (2014a).

	Northern sector (Vallès area)			
	Fault geometry	Reactivation of pre-existing fault	FAULT ZONE CHARACTERISTICS OF THE ACTIVE FAULTS	
			Fault core	Fault damage zone
Late Jurassic-Early Cretaceous extension	SE-dipping **extensional fault with two planar panels**: an upper dipping about 60º and a lower dipping less than 30º	Not observed.	**Upper fault panels:** • Decametric to hectometric thick formed by blue clay gouges with a sub-horizontal to shallow-dipping foliation and cataclasites embedding metric to decametric blocks of Paleozoic Lower and Triassic rocks. • No evidence of induced syn-kinematic cement precipitation.	**Upper fault panels:** • Paleozoic rocks cut by metric to decametric faults developed in the finest grained lithologies. • No evidence of induced syn-kinematic cement precipitation
Paleogene compression	**Upper fault reactivated panels:** Steep SE-dipping left-lateral strike-slip fault. **New formed short-cut thrusts (Pre-littoral Thrust):** ~30° SE-dipping NW-directed short-cut thrust fault.	Reactivation of the upper steep panels of the Mesozoic fault Reactivation of the low angle (~30°) panels of the Mesozoic fault.	**Upper fault reactivated panels:** Decametric to hectometric thick blue clay gouge with a nearly vertical E-trending foliation and rod-shaped ellipsoidal quartz blocks with a vertical long axis and are encircled by near-horizontal striae **New formed short-cut thrusts (Pre-littoral Thrust):** • 1 to 3-m-thick constituted by cemented (calcite) breccias and cataclasites and vertical non-cemented stylolites when developed in Triassic carbonate rocks • Foliated clay gouges with abundant shear bands and without cement precipitation when formed in metamorphic Paleozoic rocks.	**Upper fault reactivated panels:** • Not observed **New formed short-cut thrusts (Pre-littoral Thrust):** • Metric (occasionally decimetric) to decametric thick zone. • Amalgamated thrusts and deformation bands that define different scale duplexes
Late Oligocene-Neogene extension	**Vallès-Penedès Fault:** kinked SE-dipping planar fault with an upper panel dipping around 60° and a lower panel dipping less than 30°.	Partial reactivation of the upper steep panels of the Mesozoic faults Reactivation of the lower fault panel (~30°) of the Mesozoic fault and the Paleogene related short-cut thrusts.	**Upper fault panels (Vallès-Penedès Fault):** • Narrow (<5 meters). • Mud-to-clast-supported non-cemented breccias with SSE foliation. • Cataclasites cemented by chlorite and associated calcite and laumontite minerals.	**Upper fault panels (Vallès-Penedès Fault):** • Hectometric to kilometric thick zones. • **Footwall**: <100 meters wide with ENE-trending extensional faults whose intensity increases towards the fault core. • **Hangingwall**: hectometric to kilometric wide extensional fault propagation fold cut by conjugated extensional planar faults.

1998). From outcrop observations, this fault zone includes a decametric to hectometric thick fault core formed by blue clay gouges and cataclasites embedding metric to even decametric blocks of Paleozoic phyllites, wackes, granitoids and quartz veins as well as of Lower Triassic red sandstones (Julià and Santanach, 1998; Camps and Morera, 2014). The vein quartz blocks often are rod-shaped and ellipsoidal with a nearly vertical long axis and are encircled by near-horizontal striae (Anadón et al., 1985). These rods, together with the other rocks present in the fault core define a sub-vertical banding that resulted from textural variations generated by different degrees of crushing (Julià and Santanach, 1984). At a minor observation scale, the fault gouges (composed of iron-rich chlorite, illite and quartz) show a sub-horizontal to shallow south-dipping or nearly vertical E-trending foliation (Julià and Santanach, 1998; Camps and Morera, 2014). Around the fault core, the fault damage zone is constituted by Paleozoic rocks (mainly phyllites and wackes) cut by metric to decametric faults that, rather parallel to the fault core, mainly developed in the finest grained lithologies. These minor faults include a core also made up by fault gouges but with a much thinner thickness (usually <20 cm). Both in the damage zone and the fault core no evidence of induced syn-kinematic cement precipitation during their development has been described.

About the age of this fault zone, Arthaud and Matte (1975) proposed a late Hercynian age based on speculative regional criteria about western Europe-scale evolution. Anadón et al. (1985) interpreted it as developed during the Paleogene contractional stage. However, the present-day available data only indicates that it postdates the Early Triassic (age of some embedded blocks) and was active during the Paleogene compressional phase when formed the observed contractional structures. This time span could be reduced if we consider that this fault zone is restricted to the footwall of the Pre-littoral Thrust and, therefore, surely it is truncated by this last fault (Fig. 6A); a thrust that has been dated as early Eocene -Lutetian- (López-Blanco et al., 2000). In this restricted Early Triassic to early Eocene space of time, the predominant contractional deformation attests that this fault zone was active during the early stages of the regional Paleogene contractional deformation. But the presence of a sub-horizontal foliation, which denotes a horizontal extension, points out that this fault zone probably formed previously during the Mesozoic extension.

Regarding to the fault zones associated with the emplacement of the Paleogene thrust sheets, these consist of a metric (occasionally decimetric) to decametric thick zone observed along the outcropping Pre-littoral and Collbató thrusts (see thrust location in Fig. 2). Their fault core is centimetric to decametric thick and is mainly formed by foliated clay gouges with abundant shear bands that denote a thrust transport direction towards the north and, locally, towards the northwest. Around this fault core, the damage zone consists of a system of amalgamated thrusts and deformation bands that define different scale duplexes. The deformation features of these minor faults and deformation bands depend on the host lithology. When developed in metamorphic Paleozoic rocks (phyllites and wackes), deformation mainly consists of foliated fault gouges without cement precipitation. Instead, if they developed in or close to Triassic carbonate rocks, their core is formed by a 1 to 3-m-thick fault core constituted by breccias and cataclasites cemented by low-temperature calcite cement and vertical non-cemented stylolites (Cantarero et al., 2014a).

Finally, the fault zone linked to the late Oligocene-Neogene extension is placed along the Vallès-Penedès Fault. It is characterized at surface, by narrow fault cores (<5 m thick, usually <2 m) and decametric to even kilometric surrounding damage zones. The fault cores are made up of mud-to-clast-supported non-cemented breccias with a broad shallow SSE foliation, and, towards the ENE, also by cataclasites cemented by chlorite and associated calcite and laumontite minerals (Cantarero et al., 2014a). In the footwall, formed by Paleozoic rocks, the damage zone is <100 m-wide (Cantarero et al., 2014a) and consists of ENE-trending extensional faults with fractures that significantly increases their presence as approaching to the fault core. In the hangingwall, at surface, only Miocene deposits filling the Vallès-Penedès crop out. These syn-extensional deposits close to the fault are deformed in a hectometric to kilometric wide syncline cut by conjugated extensional planar faults with a) a <5 m displacement, b) a foliation parallel to bedding planes faults; and c) a bisector of minor angle that is always perpendicular to the bedding regardless its dip attitude (Fig. 6). So, they are affected by a fold with a bed-parallel stretching. In this scenario, the increase of both the bedding dip and faulting related bedding parallel stretching as approaching to the main fault suggest that this deformation records the development of an extensional propagation fold at the top of the moving Vallès-Penedès Fault.

3.3.2. Central sector (Penedès area)

The geometric, deformational, and petrological characteristics of the central sector of the MVFS are summarized in the Table 2. In this sector, the MVFS developed over a host-rock or protolith mostly formed, at depth, by metasedimentary siliciclastic Variscan basement. At shallower levels, instead, the host-rock is formed by a thin Triassic to Lower Jurassic succession with carbonate, siliciclastic and evaporite rocks overlain by a thicker Cenozoic syn-kinematic siliciclastic cover (sector B in Fig. 5). The presence of relatively thick pre-kinematic Middle to Upper Triassic evaporite and mudstone layers resulted in the formation of drape and fault-propagation folds above the MVFS (Marín et al., 2021). These folds absorbed part or all the motion of the underlying basement faults, delayed their upwards propagation and, therefore, prevented or hampered the observation and recognition at surface of the fault zones related to the motion of the MVFS. Additionally, post-rift Pliocene and Quaternary sediments frequently cover Mesozoic and late Oligocene-Neogene extensional faults (Gallart, 1981), which makes difficult the study of this area.

Despite these limitations, the fault zones related to the emplacement of the Paleogene short-cuts (thrusts) are still easily recognizable at surface in this central sector. Moreover, few key aspects that characterize these extensional fault zones in limited areas where faults crop out. This is the case of the Guardiola de Font-Rubí outcrop, where the Vallès-Penedès Fault crops out affecting Lower Cretaceous limestones. The fault zone developed during its Mesozoic motion is characterized by 1) a metric to, occasionally, decametric fault core made by calcite cemented breccias with abundant tension veins; and 2) a damage zone including minor NNW-trending extensional faults filled by calcite (Baqués et al., 2012). All these deformed rocks are also cut by minor ENE-trending reverse and strike-slip faults filled by calcite cements and randomly oriented stylolites (i.e., stylobreccia) (Amigó, 1984; Baqués et al., 2012). These contractional fractures have been related to the Paleogene contractional stage (Amigó, 1984; Baqués et al., 2012) and could suggest a reactivation of the previous Mesozoic extensional fault.

The clearest Paleogene fault zones in the central zone of the MVFS are the ones developed at the Paleogene short-cuts/thrusts. These crop out along the Els Brucs Thrust trace (Fig. 2) and consist of narrow fault zones with similar features to the ones described in the thrusts in the Northern sector (see Section 3.3.1).

The fault damage zone developed during the late Oligocene-Neogene extension has only been characterized in the southern half of the central sector of the MVFS, area where thick Mesozoic carbonates constitutes the protolith and the Vallès-Penedès Fault splits into two parallel faults: Foix and Les Torres faults (Amigó, 1984) (Fig. 2). In both cases, the core of the Neogene fault is metric to exceptionally decametric wide and is mainly formed by calcite-cemented fault breccias that are affected by calcite-filled tension fractures (Baqués et al., 2012). The damage zone consists of nearly vertical calcite-cemented tension fractures and high-angle extensional faults (Amigó, 1984; Baqués et al., 2012) whose density increases to the fault core.

3.3.3. Southern sector (Montmell area)

The geometric, deformational, and petrological characteristics of the southern sector of the MVFS are summarized in the Table 3. Here, the

Table 2
Characteristics of the central sector (Penedès area) of the Montmell-Vallès Fault System. Compiled from Amigó (1984) and Baqués et al. (2012).

	Central sector (Penedès area)			
	Fault geometry	Reactivation of pre-existing fault	FAULT ZONE CHARACTERISTICS OF THE ACTIVE FAULTS	
			Fault core	Fault damage zone
Late Jurassic-Early Cretaceous extension	SE-dipping fault with two planar panels: one dipping around 60° and a lower dipping less than 30°.	Not observed.	**Upper fault panels:** • Metric to, occasionally, decametric thick. • Calcite cemented breccias with abundant tension veins.	**Upper fault panels:** • Minor NNW-trending extensional faults filled by calcite
Paleogene compression	**New formed short-cut thrusts (Els Brucs and Gaià-El Camp thrusts):** ~30° SE-dipping NW-directed short-cut thrusts.	Reactivation of the lower low angle (~30°) fault panel.	**New formed short-cut thrusts (Els Brucs Thrust):** • 1 to 3-m-thick constituted by cemented (calcite) breccias and cataclasites and vertical non-cemented stylolites when developed in Triassic carbonate rocks • Foliated clay gouges with abundant shear bands and without cement precipitation when formed in metamorphic Paleozoic rocks.	**Upper fault panels:** • Not studied/observed **New formed short-cut thrusts:** • Metric (occasionally decimetric) to decametric thick zone. • Amalgamated thrusts and deformation bands that define different scale duplexes.
Late Oligocene-Neogene extension	**Vallès-Penedès, fault Les Torres and Foix faults:** SE-dipping extensional fault with two planar panels: an upper steep with a dip of about 60º and a lower one that dips less than 30º.	Reactivation of the lower panel of the Mesozoic fault as well as of some segments of the Paleogene short-cut thrusts.	**Upper fault panels (Vallès-Penedès Fault):** • Metric to exceptionally decametric wide fault core mainly formed by calcite-cemented fault breccias that are affected by calcite-filled tension fractures.	**Upper fault panels (Vallès-Penedès Fault):** • Nearly vertical calcite-cemented tension fractures and high-angle extensional faults whose density increases to the fault core.

Table 3
Characteristics of the southern sector (Montmell area) of the Montmell-Vallès Fault System. Compiled from Belaid et al. (2008), Baqués et al. (2010, 2012, 2014) and Marín et al. (2021).

	Southern sector (Montmell area)			
	Fault geometry	Reactivation of pre-existing fault	FAULT ZONE CHARACTERISTICS OF THE ACTIVE FAULTS	
			Fault core	Fault damage zone
Late Jurassic-Early Cretaceous extension	kinked SE-dipping fault with an upper panel of around 60° and a lower panel of around 30°.	Not observed.	**Upper fault panels:** • Narrow fault core made up of carbonate breccias cut by tension fractures and extensional faults.	**Upper fault panels:** • **Hangingwall**: small-scale calcite-cemented extensional faults.
Paleogene compression	**New formed short-cut thrusts (Gaià-El Camp Thrust):** ~30° SE-dipping NW-directed short-cut thrusts.	Contractional reactivation of the lower low angle (~30°) fault panel.	*Fault zones cannot be characterized by surface observations.*	
Late Oligocene-Neogene extension	**New formed extensional short-cut faults (Baix Penedès Fault):** SE-dipping extensional fault with two planar panels: an upper one steep with a dip of about 60º and a lower one that dips less than 30º.	Extensional reactivation of the lower low angle (~30°) fault panel.	**Upper fault panels (Montmell Fault):** • Carbonate fault-core-related breccias and cataclasites that are cut by second-order extensional faults. • Cohesive fault core due to the presence of different generations of calcite cement, which strengthen and heal breccias and cracks.	**Upper fault panels (Montmell Fault):** • Nearly vertical calcite-cemented tension fractures and high-angle extensional faults

upper panels of the faults of the MVFS developed over a host-rock or protolith similar to the one in the central sector but with a thicker post-Triassic carbonate succession (sector C in Fig. 5). Also, it is a sector in which there is relatively thick pre-kinematic Middle to Upper Triassic evaporite and mudstone layers in the host-rock resulting in the formation of drape and fault-propagation folds above the MVFS (Marín et al., 2021).

Compared to the other two sectors, the reactivation of the upper panels of the Mesozoic faults of the MVFS is practically non-existent. As shown in the Marmellar section in Fig. 6, the only outcropping Mesozoic fault (the Montmell Fault) did not move during both Paleogene compressional and late Oligocene-Neogene extensional stages.

At the studied outcrops, this Mesozoic fault has a narrow fault core made up of carbonate breccias cut by tension fractures and extensional faults, and a damage zone that, in its hangingwall, is characterized by small-scale calcite-cemented extensional faults that have been rotated/folded during the Paleogene contractional deformation (i.e., Riera del Marmellar outcrop, Baqués et al., 2012) (Fig. 6B). This last contractional deformation did not reactivate the Mesozoic fault but generated in its hangingwall buttressing structures that include folds, thrusts and small-

scale backthrusts with a core constituted by centimetric to decametric-thick cohesive cataclasites (Fig. 6B).

Therefore, the development of major Paleogene contractional stage-related fault zones in this sector appears restricted to the formation of the shortcuts at the footwall of the Mesozoic faults. The features of fault zones, however, cannot be characterized by surface geology. As shown in Fig. 2, the major Paleogene structure does not crop at surface as this and its related fault zones are buried beneath the decoupled Triassic cover that, covering the entire area, absorbed the basement fault motions forming drape and propagation folds (Fig. 3ii).

Finally, as concern to the late Oligocene-Neogene extension, the only major related fault zone present in this sector is the one linked to the formation of the Baix Penedès Fault. It is a > 300-m-wide fault zone formed by carbonate fault-core-related breccias and cataclasites that are cut by second-order extensional faults (Baqués et al., 2010, 2014). As the rest of the faults developed over a thick carbonate protolith in this and the central sectors of the MVFS, it is a relatively cohesive fault zone due to the presence of different generations of calcite cement, which strengthen and heal breccias and cracks (Belaid et al., 2008; Baqués et al., 2014).

3.4. Controls on the Montmell-Vallès Fault extensional reactivation during the Neogene

The Montmell-Vallès Fault System shows similar kinked-planar geometry all along its trace. From a geometry point of view, the most significant difference is the change of its SE dip from >60° in the shallower parts (present-day limit of the Neogene basin) to 30° at depth. The deepest and less dipping part of the fault would most likely correspond to the continuation of the Paleogene thrust at depth (the Pre-littoral Thrust in the northern sector and the Gaià-El Camp Thrust in the central and southern sectors; Fig. 3) (Marín et al., 2021). The basal detachment of the VMFS would correspond to the top of the reflective crust located in the central CCR between 13 and 16 km depth (Fernàndez and Banda, 1990; Sàbat et al., 1997; Roca et al., 2004). Considering the described geometry and the fact that the orientation of the stress field across the region has been defined as constant during the Neogene extension (Bartrina et al., 1992; Herraiz et al., 2000), differences in Neogene reactivation cannot only be explained by variations in the local stress due to changes in the fault plane orientation and dip. Hence, the inherited rheology of the pre-existent Mesozoic and Paleogene fault rocks, and the effect of mineralizations and cementations within the fault zone due to fluid circulation during previous tectonic phases should be considered as a factor to explain the different reactivation.

Extensional reactivation of the Montmell-Vallès Fault System during the Neogene principally took place in areas where the host-rock was essentially siliciclastic, and the pre-existent fault core developed a non-cohesive gouge. In these cases, pre-existent fault rocks appear weaker than the host-rock and, therefore, the fault core can be easily reactivated. On the other hand, fault reactivation appears restricted or even absent in sectors where the host-rock included thick carbonate successions and pre-existent fault rocks consisted in well-cemented cohesive carbonate breccias. Precipitation of calcite cements and other minerals along fault zones is described as a mechanism that enlarge fracture-wall adherence increasing fault rock strength and shifting the failure envelope to higher values (Li et al., 2003; Ferrill and Morris, 2008; Hausegger et al., 2010; Ferrill et al., 2011; Hooker et al., 2012). In our case this would imply that fault breccias developed along the Montmell-Vallès Fault System were already cemented and without fluids when Neogene reactivation initiated. In those cases, pre-existent fault rocks would be welded to the host-rock by this cementation showing homogeneous rock strength and, consequently, the pre-existent fault plane did not play as an inherited weakness. These facts agree with other investigations carried out along the Vallès-Penedès Fault (e.g., Travé et al., 1998; Belaid et al., 2008) and other Neogene faults in the CCR (Cantarero et al., 2014b, 2018), which basically show that precipitation and crystallization of carbonates seal fault planes either blocking their reactivation or decreasing the capacity of sliding of the fault during deformation.

The change of fault rock mechanical properties due to mineralizations and/or cementations (e.g., calcite precipitation) within the observed fault zones along the three sectors of the Vallès-Penedès Fault would explain such differences in the Neogene reactivation. Although the three sectors present siliciclastic rocks from the Variscan basement and the Triassic, only part of the central sector and the southern one present a well-developed Mesozoic carbonate cover that would have enhanced the development of a cohesive fault breccia (Fig. 6). Regardless the presence of relatively thin Triassic carbonate host-rock and the precipitation of calcite in the fault zone in the northern sector of the Vallès-Penedès Fault during the Mesozoic (Cantarero et al., 2014a) (Fig. 5), rock strength did not increase in this sector and reactivation occurred smoothly. Reactivation in the northern sector might be also supported by the presence of a silicate-rich fault gouge, which would have reduced fault strength and the coefficient of friction (Wang et al., 1980; Wintsch et al., 1995; Alder et al., 2016) (Fig. 5) facilitating fault slip at the end of the Paleogene compression.

The Neogene reactivation in the southern sector of the Montmell-Vallès Fault System must consider fluid/host-rock interactions when such reactivation began (late Oligocene-early Miocene). With this regard, considering the current hydrologic system, fault gouges probably acted as fluid flow paths and, consequently, were already zones of weakness. Additionally, published petrological and geochemical analysis in fault breccias (i.e., Baqués et al., 2012) show that, at the end of the Paleogene compression, these areas corresponded to systems with very low or non-existent permeability and, therefore, areas with very low fluid pressure and higher strength.

The Montmell Fault damage zone has been characterized by conductive rocks (Marín et al., 2021), that suggest the presence of fluids. This fact appears opposite to the idea of the restricted reactivation observed of the southern sector during the Neogene extension due to fault sealing. However, the conductive body is 2 km deep, a depth at which Variscan rocks are present in both fault-walls. Therefore, it seems more likely to be associated with the presence of fault gouges in which hydrothermal activity is present like in the northern sector of the fault. In the northern sector, fluid circulation can be considered either synchronic to or post fault movement.

The rheology of fault rocks backed the reactivation of the Mesozoic fault in areas where primarily the Variscan basement was involved in the deformation. Conversely, this reactivation appears difficult or restricted in areas where a relatively thick carbonate-rich Mesozoic cover is present. The three sectors of the Montmell-Vallès Fault System followed different degrees of reactivation linked to these restrictions and a differential growth and evolution of the fault zones. In the northern sector, the upper panels of the fault essentially involved basement rocks at the onset of the extension and a weak fault gouge developed. In the northern part of central sector, the shallower part of the fault includes well-cemented and cohesive fault breccia that appears insufficient (possibly too short or too thin) and to compensate for the weakness of the underlying fault gouge. Instead in the southern sector, the portion of the fault with well-developed and cemented breccias appears longer, and possibly wider, which seems capable of restraining or even completely blocking the reactivation of the underlying weak fault gouge.

4. Conclusions

The synthesis from previous works and the analysis of the structural styles and the fluid-rock interactions present along the trace of the Mesozoic-inherited Montmell-Vallès Fault System allows discerning between different degrees of reactivation of this major fault during the Cenozoic. The Montmell-Vallès Fault System can be divided into three main sectors (northern, central, and southern) considering their response during the main tectonic stages affecting the area since the

Mesozoic (Late Jurassic to Early Cretaceous extension, Late Cretaceous to late Oligocene compression, and Latest Oligocene(?)/early late Miocene extension).

A period of positive tectonic inversion and contractional reactivation related to the Paleogene compressional phase is attested by the presence of highly deformed areas (thin-skinned thrusting and footwall shortcut development) along the footwall of the Montmell-Vallès Fault System. However, reactivation of the Montmell-Vallès Fault System appears decoupled. Whereas the lower part of the fault does reactivate in (almost) all its length, the reactivation of the upper part is restricted to areas with thick carbonate protoliths where faulting resulted in the formation of well calcite-cemented fault rocks (breccias) due to fluid circulation during the Mesozoic extensional phase (i.e., central, and southern sectors). The development of well-cemented fault rocks would have increased fault strength and the coefficient of friction limiting such reactivations and, hence, triggering the propagation of the deformation to the fault footwall resulting in shortcut formation. The Gaià-El Camp, Els Brucs, and Pre-littoral thrusts correspond to major footwall shortcuts that uplifted the footwall of the Montmell-Vallès Fault over the Ebro Basin during the compression. The positive tectonic inversion of the Montmell-Garraf Basin produced the exhumation and erosion of part of the Mesozoic cover, the current NE limit of which lies around 10 km SW of the Llobregat River.

The negative inversion of the Montmell-Vallès Fault System during the early to late Miocene extension appears also governed by inherited fault zone anisotropies when the extension began. Reactivation decoupling between the upper and lower parts of the fault also occurred. Whereas, the deeper part was reactivated along all the Montmell-Vallès Fault trace, the high dipping and shallower part experienced different degrees of reactivation. The likelihood of the fault to be reactivated appears highly controlled by 1) the lithology of the host-rock that characterizes fault rock types and locations, 2) the formation of fault rocks in presence of fluids (cementation) during the main fault activity, and 3) the change of the mechanical properties of fault rocks which in turn governs the ability of the fault to be reactivated.

Reactivation was very effective in areas where the host-rock was composed by granitoids and siliciclastic metasediments (i.e., Variscan basement), and the pre-existent fault core was an impermeable and non-cohesive gouge (i.e., northern sector). Yet, fault reactivation was restricted, or even prevented, in areas where the host-rock and the pre-existing fault core included respectively thick carbonate successions and highly cemented and cohesive breccias. Taking into consideration that the central and the southern sectors present similar host-rocks (both constitute the NW limit of an extensional basin filled-up with relatively thick carbonate successions during the Mesozoic), the causes of the different reactivations remain uncertain. These differences seem rather related to the size (height and width) of the cemented breccias in the inherited fault zone, which would increase towards the SW preventing (or limiting) fault reactivation in the southern sector and shifting the extension towards the SE along the Baix Penedès Fault.

Declaration of Competing Interest

The authors declare that they have no known competing financial interests or personal relationships that could have appeared to influence the work reported in this paper.

Data availability

No data was used for the research described in the article.

Acknowledgements

This research was carried out within the framework of DGICYT Spanish Projects DGICYT PID2021-122467NB-C22, PID2020-117598 GB-I00, PID2019-106440GB-C21 and PGC2018-093903-B-C22 (Ministerio de Ciencia, Innovación y Universidades/Agencia Estatal de Investigación / Fondo Europeo de Desarrollo Regional, Unión Europea), and the SABREM Project PID2020-117598GB-I00 funded by MCIN/ AEI /10.13039/501100011033. The Grups Consolidats de Recerca "Geologia Sedimentària" (2017-SGR-824) and "Geodinàmica i Anàlisi de Conques" (2017-SGR467) of the Generalitat de Catalunya, and the UB-Geomodels Research Institute are also acknowledged. Constructive reviews from an anonymous reviewer (AB) and Françoise Roure significantly improved the original manuscript, for which the authors are very thankful. Fadi H. Nader is also thanked for his comments and recommendations and for his role as journal editor.

References

Agosta, F., Aydin, A., 2006. Architecture and deformation mechanism of a basin-bounding normal fault in Mesozoic platform carbonates, Central Italy. J. Struct. Geol. 28, 144.

Agustí, J., Cabrera, L., Moya, S., 1985. Sinopsis estratigráfica del Neógeno en la fosa del Vallès-Penedès. Paleontología Evolutiva 18, 57–81.

Albrich, S., Bernaus, J.M., Boix, C., Caus, E., Martín-Closas, C., Salas, R., Vicedo, V., Villalonga, R., 2006. Caracterización bioestratigráfica y paleoambiental del Cretácico Inferior (Berriasiense-Barremiense) del Macizo de Garraf (Cadena Costera Catalana). Rev. Esp. Micropaleontol. 38 (2–3), 429–451.

Aldega, L., Viola, G., Casas-Sainz, A., Marcen, M., Roman-Berdiel, T., van der Lelij, R., 2019. Unraveling multiple thermotectonic events accommodated by crustal-scale faults in Northern Iberia, Spain: insights from K-Ar dating of clay gouges. Tectonics 38, 3629–3651.

Alder, S., Smith, S.A.F., Scott, J.M., 2016. Fault-zone structure and weakening processes in basin-scale reverse faults: the moonlight fault zone, South Island, New Zealand. J. Struct. Geol. 91, 177–194.

Almera, J., 1894. Descripción de los terrenos pliocénicos de la cuenca del Bajo Llobregat y llano de Barcelona. In: Mem. R. Acad. Cienc. y Art. Barcelona, 3ª Época, pp. 1–102. Barcelona.

Amigó, J., 1984. La falla del Valles-Penedes entre Pontons y Font-Rubí (Alt-Penedès). Acta Geol. Hisp. 19, 1–4.

Amilibia, A., McClay, K., Sàbat, F., Muñoz, J.A., Roca, E., 2005. Analogue modelling of inverted oblique rift systems. Geol. Acta 3 (3), 251–271.

Anadón, P., 1978. El Paleógeno continental anterior a la transgresión Biarritziense (Eoceno medio) entre los ríos Gaia y Ripoll (prov. de Tarragona y Barcelona). Estud. Geol. 34, 341–440.

Anadón, P., 1986. Las facies lacustres del Oligoceno de Campins (Vallés oriental, provincial de Barcelona). Sedimentación continental de España. Cuadernos de Geología Ibérica 10, 271–294.

Anadón, P., Colombo, F., Esteban, M., Marzo, M., Robles, S., Santanach, P., Solé-Sugrañes, L., 1979. Evolución tectonoestratigráfica de los Catalánides. Acta Geol. Hisp. 14, 242–270.

Anadón, P., Cabrera, Ll, Guimerà, J., Santanach, P., 1985. Paleogene strike-slip deformation and sedimentation along the southeastern margin of the Ebro Basin. In: Biddle, K.T., Christie-Blick, N. (Eds.), Strike-Slip Deformation, Basin Formation and Sedimentation, Society of Economic Paleontologists and Mineralogists Special Publication, 37, pp. 301–318.

Angrand, P., Mouthereau, F., 2020. Evolution of the Alpine orogenic belts in the Western Mediterranean region as resolved by the kinematics of the Europe-Africa diffuse plate boundary. BSGF - Earth Sci. Bull. 192 (42), 44.

Arnal, I., Calvet, F., Márquez, L., Márquez-Aliaga, A., Solé de Porta, N., 2002. La plataforma carbonatada epeírica (Formaciones Imón e Isábena) del Triásico superior del Noreste de la Península Ibérica. Acta Geol. Hisp. 37 (4), 299–328.

Arthaud and Matte, 1975. Les décrochements tardi-hercyniens du sud-ouest de l'Europe. Géométrie et essai de reconstitution des conditions de la déformation. Tectonophysics 25 (1–2), 139–171.

Ashauer, H., Teichmüller, R., 1935. Die variszische und alpidische Gebirgsbildung Kataloniens. Abhandlungen Gesellschaft Wissenschaften Göttingen. Theor. Math. Phys. K1 (3F), 16.

Aydin, A., Myers, R., Younes, A., 1998. Faults: seals or migration pathways? Yes, no, some are but some aren't, and some faults are but only sometimes! AAPG Ann. Conv. A37, 5–1467.

Bailey, W.R., Walsh, J.J., Manzocchi, T., 2005. Fault populations, strain distribution and basement fault reactivation in the East Pennines Coalfield, UK. J. Struct. Geol. 27 (913), 928.

Baqués, V., Travé, A., Benedicto, A., 2008. Relación entre circulación de fluidos y brechificación en la cuenca extensiva neógena del Penedès (NE Península Ibérica). Geotemas 10, 1437–1440.

Baqués, V., Travé, A., Benedicto, A., Labaume, P., Cantarero, I., 2010. Relationships between carbonate fault rocks and fluid flow regime during propagation of the Neogene extensional faults of the Penedès basin (Catalan Coastal Ranges, NE Iberian). J. Geochem. Explor. 106, 24–33.

Baqués, V., Travé, A., Roca, E., Marín, M., Cantarero, I., 2012. Geofluid behavior in successive extensional and compressional events: a case study from the southwestern end of the Vallès-Penedès Fault (Catalan Coastal Ranges, NE Spain). Pet. Geosci. 18 (2012), 17–31.

Baqués, V., Travé, A., Cantarero, I., 2014. Development of successive karstic systems within the Baix Penedès Fault zone (onshore of the Valencia Trough, NW Mediterranean). Geofluids 14, 75–94.
Barberà, X., Cabrera, L., Marzo, M., Parés, J.M., Agustí, J., 2001. A complete terrestrial Oligocene magnetostratigraphy from the SE Ebro foreland basin, NE Spain. Earth Planet. Sci. Lett. 187, 1–16.
Bartrina, M.T., Cabrera, L., Jurado, M.J., Guimerà, J., Roca, E., 1992. Evolution of the central margin of the Valencia trough (western Mediterranean). Tectonophysics 203, 219–247.
Belaid, S., Baqués, V., Travé, A., Benedicto, A., Plagnes, V., 2008. El karst de la falla del Vallés-Penedés (NE de España). Geotemas 10, 429–432.
Belenguer, J., Roca, E., Gratacós, O., 2012. Evidencias de una rampa de relevo extensivo de edad miocena en el sector del Baix Llobregat de la falla del Vallès-Penedès, Cataluña. In: Fernández, L.P., Fernández, A., Cuesta, A., Bahamonde, J.R. (Eds.), Geo-Temas 13: Resúmenes extendidos del VIII Congreso Geológico de España, pp. 141–144.
Bois, C., 1992. The evolution of the layered lower crust and Moho through Geological time in Western Europe: contribution of deep seismic reflection profiles. Terra Nova 4, 99–108.
Bond, R.M.G., McClay, K.R., 1995. Inversion of lower cretaceous extensional basin, south Central Pyrenees, Spain. In: Buchanan, J.G., Buchanan, P.G. (Eds.), Basin Inversion, 88. Geological Society Special Publication, pp. 415–431.
Bonini, M., Sani, F., Antonielli, B., 2012. Basin inversion and contractional reactivation of inherited normal faults: a review based on previous and new experimental models. Tectonophysics 522-523, 55–88.
Buatier, M., Lacroix, B., Labaume, P., Moutarlier, V., Charpentier, D., Sizun, J.P., Travé, A., 2012. Microtextural investigation (SEM and TEM study) of phyllosilicates in a major thrust fault zone (Monte Perdido, southern Pyrenees): impact on fault reactivation. Swiss J. Geosci. 105, 313–324.
Buchanan, J.G., Buchanan, P.G., 1995. Basin Inversion, 88. Geological Society Special Publication, p. 596.
Butler, R.W.H., 2017. Basement-cover tectonics, structural inheritance, and deformation migration in the outer parts of orogenic belts: a view from the western Alps. In: Law, R.D., Thigpen, J.R., Merschat, A.J., Stowell, H.H. (Eds.), Linkages and Feedbacks in Orogenic Systems: Geological Society of America Memoir, p. 213.
Butler, R., Tavarnelli, E., Grasso, M., 2006. Tectonic inversion and structural inheritance in mountain belts. J. Struct. Geol. 28, 1891–1892.
Cabrera, L., Calvet, F., 1996. Onshore Neogene record in NE Spain: Vallès-Penedès and El Camp half-grabens (NW Mediterranean). In: Friend, P.T., Dabrio, D. (Eds.), Tertiary Basins of Spain, pp. 97–105.
Cabrera, L., Roca, E., Garcés, M., de Porta, J., 2004. Estratigrafía y evolución tectonosedimentària oligocena superior-neógena del sector central del margen catalán (Cadena Costero Catalana). In: Vera, J.A. (Ed.), Cuencas Cenozoicas. Geologia de España. SGE-IGME, pp. 569–572.
Calvet, F., Marzo, M., 1994. El Triásico de las Cordilleras Costero Catalanas: estratigrafía, sedimentología y análisis secuencia. In: Field guide III Coloquio de Estratigrafía y Sedimentología del Triásico y Pérmico de España, pp. 1–53.
Calvet, F., Travé, A., Roca, E., Soler, A., Labaume, P., 1996. Fracturación y migración de fluidos durante la evolución tectónica neógena en el Sector Central de las Cadenas Costeras Catalanas. Geogaceta 20 (7), 1715–1718.
Calvet, F., Canals, A., Cardellach, E., Carmona, J.M., Gómez-Gras, D., Parcerisa, D., Bitzer, K., Roca, E., Travé, A., 2000. Fluid migration and interaction in extensional basins: application to the Triassic and Neogene rift in the central part of the Catalan Coastal Ranges, NE Spain. In: Field Guide III Geofluids Congress, p. 58.
Calvet, F., Travé, A., Bitzer, K., Roca, E., Tritlla, J., Baker, J., 2001. Dolomitization of detrital deposits related to Neogene extensional faults, Catalan Coastal Ranges (Spain). Geo-Temas 3 (1), 109–111.
Camps, I., Morera, D., 2014. Caracetrització i significat estructural d'un aflorament Paleozoic inèdit situat a la llera de la riera de les Arenes (Matadepera, Vallès Occidental). In: VIII Trobada d'Estudiosos de Sant Llorenç del Munt i l'Obac. Barcelona 2014.
Cantarero, I., Travé, A., Alías, G., Baqués, V., 2010. Pedogenic products sealing normal faults (Barcelona Plain, NE Spain). J. Geochem. Explor. 106, 44–52.
Cantarero, I., Lanari, P., Vidal, O., Alias, G., Travé, A., Baqués, V., 2014a. Long-term fluid circulation in extensional faults in the central Catalan Coastal Ranges: P-T constraints from neoformed chloride and K-white mica. Int. J. Earth Sci. 103, 165–188.
Cantarero, I., Travé, A., Alías, G., Baqués, V., 2014b. Polyphasic hydrothermal and meteoric fluid regimes during the growth of a segmented fault involving crystalline and carbonate rocks (Barcelona Plain, NE Spain). Geofluids 14, 20–44.
Cantarero, I., Zafra, C.J., Travé, A., Martín-Martín, J.D., Baqués, V., Playá, E., 2014c. Fracturing and cementation of shallow buried Miocene proximal alluvial fan deposits. Mar. Pet. Geol. 55, 87–99.
Cantarero, I., Alías, G., Cruset, D., Carola, E., Lanari, P., Travé, A., 2018. Fluid composition changes in crystalline basement rocks from ductile to brittle regimes. Glob. Planet. Chang. 171, 273–292.
Cantarero, I., Parcerisa, D., Plata, M.A., Gómez-Gras, D., Gomez-Rivas, E., Martín-Martín, J.D., Travé, A., 2020. Fracturing and near-surface diagenesis of a silicified miocene deltaic sequence: the Montjuïc Hill (Barcelona). Minerals 10 (2), 135.
Cardellach, E., Canals, À., Grandia, F., 2002. Recurrent hydrothermal activity induced by successive extensional episodes: the case of the Berta F-(Pb-Zn) vein system (NE Spain). Ore Geol. Rev. 22, 133–141.
Carminati, E., Wortel, M.J.R., Meijer, P.T., Sabadini, R., 1998. The two-stage opening of the western-Central Mediterranean basins: a forward modeling test to a new evolutionary model. Earth Planet. Sci. Lett. 160, 667–679.
Colombo, F., 1986. Continental Paleogene stratigraphy and sedimentology of the western southern border of the Catalanides, Tarragona Province, Spain. Cuadernos de Geología Ibérica 10, 55–115.
Cooper, M.A., Williams, G.D., de Granciasnky, P.C., Murphy, R.W., Needham, T., de Paor, D., Stonley, R., Todd, S.P., Turner, J.P., Ziegler, P.A., 1989. Inversion Tectonics – A discussion. In: Cooper, M.A., Williams, G.D. (Eds.), Inversion Tectonics. Special Publication of the Geological Society of London, 44. Blackwell Scientific Publications, pp. 335–347.
Corregidor, J., Cabrera, L., Parés, J.M., 1997. Magnetoestratigrafía de las sucesiones pliocénicas del Baix Llobregat: aproximación preliminar. Acta Geol. Hisp. 32 (3–4), 147–160.
Dañobeitia, J.J., Arguedas, M., Gallart, F., Banda, E., Makris, J., 1992. Deep crustal configuration of the Valencia Trough and its Iberian and Balearic borders from extensive refraction and wide-angle reflection profiling. Tectonophysics 203, 37–55.
Durán, H., Julivert, M., 1990. Estratigrafía paleozoica de la parte norte y central de las Cadenas Costeras Catalanas (NE España). Acta Geol. Hisp. 25 (1–2), 3–12.
Enrique, P., 1990. The Hercynian intrusive rocks of the Catalonian Coastal Ranges (NE Spain). Acta Geol. Hisp. 25, 39–64.
Enrique, P., Solé, J., 2004. El basamento ígneo. Las rocas intrusivas de la Cordillera Costero-Catalana. In: Vera, J.A. (Ed.), Geología de España. SGE-IGME, Madrid, pp. 481–484.
Escudero-Mozo, M.J., Márquez-Aliaga, A., Goy, A., Martín-Chivelet, J., López-Gómez, J., Márquez, L., Arche, A., Plasencia, P., Pla, C., Marzo, M., Sánchez-Fernández, D., 2017. Middle Triassic carbonate platforms in eastern Iberia: evolution of their fauna and palaeogeographic significance in the western Tethys. Palaeogeogr. Palaeoclimatol. Palaeoecol. 417, 236–260.
Esteban, M., Julià, R., 1973. Discordancias erosivas intrajurásicas en los Catalánides. Acta Geol. Hisp. 8, 153–157.
Esteban, M., Robles, S., 1976. Sobre la paleogeografía del Cretácico Inferior de los Catalánides entre Barcelona y Tortosa. Acta Geol. Hisp. XI, 73–78.
Fernàndez, M., Banda, E., 1990. Geothermal anomalies in the Vallès-Penedès Graben Master Fault: convection through the horst as a possible mechanism. J. Geophys. Res. 95 (B4), 4887–4894.
Ferrer, J., 1971. El Paleoceno y Eoceno del borde suroriental de la Depresión del Ebro (Cataluña). Memories Suisses de Paléontologie 90, 70.
Ferrer, O., McClay, K.R., Sellier, N.C., 2016. Influence of fault geometries and mechanical anisotropies on the growth and inversion of hanging-wall synclinal basins: insights from sandbox models and natural examples. Geol. Soc. Lond., Spec. Publ. 439, 487–509.
Ferrill, D.A., Morris, A.P., 2008. Fault zone deformation controlled by carbonate mechanical stratigraphy, Balcones fault system, Texas. AAPG Bull. 92-3, 359–380.
Ferrill, D.A., Morris, A.P., McGinnis, R.N., Smart, K.J., Ward, W.C., 2011. Fault zone deformation and displacement partitioning in mechanically layered carbonates: the Hidden Valley fault, Central Texas. AAPG Bull. 95-8, 1383–1397.
Fontboté, J.M., 1954. Las relaciones tectónicas de la depresión del Vallés-Penedés con la Cordillera Prelitoral Catalana y con la Depresión del Ebro. In: Tomo Homenaje a Prof. E. Hernández-Pacheco, Madrid. Real Sociedad Española de Historia Natural, pp. 281–310.
Fontboté, J.M., Guimerà, J., Roca, E., Sabat, F., Santanach, P., Fernández-Ortigosa, F., 1990. The Cenozoic geodynamic evolution of the Valencia trough (western Mediterranean). Rev. Soc. Geol. Esp. 3 (3–4), 249–259.
Fossen, H., 2020. Fault classification, fault growth and displacement. In: Regional Geology and Tectonics: Principles of Geologic Analysis. Chapter 8. Elsevier. https://doi.org/10.1016/B978-0-444-64134-2.00007-9.
Galán-Abellán, B., López-Gomez, J., Berrenechea, J.F., Marzo, M., De la Horra, R., Arche, A., 2013. The beginning of the Buntsandstein cycle (Early-Middle Triassic) in the Catalan Ranges, NE Spain: sedimentary and palaeogeographic implications. Sediment. Geol. 296, 86–102.
Gallart, F., 1981. Neógeno superior y Cuaternario del Penedés (Catalunya, España). Acta Geol. Hisp. 16, 151–157.
Garcés, M., López-Blanco, M., Valero, L., Muñoz, J.A., Oliva-Urciae, B., Vinyoles, A., Arbués, P., Cabello, P., Cabrera, L., 2020. Paleogeographic and sedimentary evolution of the south Pyrenean foreland Basin. Mar. Pet. Geol. 113, 104105.
García-Senz, J., Pedrera, A., Ayala, C., Ruiz-Constan, A., Robador, A., Rodriguez-Fernández, L.R., 2019. Inversion of the north Iberian hyperextended margin: the role of exhumed mantle indentation during continental collision. Geol. Soc. Spec. Publ. 490, 177–198.
Gaspar-Escribano, J., García-Castellanos, D., Roca, E., Cloetingh, S., 2004. Cenozoic vertical motions of the Catalan Coastal Ranges (NE Spain): the role of tectonics, isostasy, and surface transport. Tectonics 23, 1–18.
Gil Ibarguchi, J.I., Julivert, M., 1988. Petrología de la aureola metamórfica de la granodiorita de Barcelona en la Sierra de Collserola (Tibidabo). Estud. Geol. 44, 353–374.
Gómez, M., Guimerà, J., 1999. Estructura Alpina de la Serra de Miramar y del NE de las Muntanyes de Prades (Cadena Costera Catalana). Rev. Soc. Geol. Esp. 12 (3–4), 405–418.
Gómez-Gras, D., Parcerisa, D., Bitzer, K., Calvet, F., Roca, E., Thiry, M., 2000. Hydrogeochemistry and diagenesis of Miocene sandstones at Montjuïc, Barcelona (Spain). J. Geochem. Explor. 69-70, 177–182.
Gómez-Gras, D., Parcerisa, D., Calvet, F., Porta, J., Solé de Porta, N., Civís, J., 2001. Stratigraphy and petrology of the Miocene Montjuïc delta (Barcelona, Spain). Acta Geol. Hisp. 36 (1–2), 115–136.
Gong, Z., Langereis, C.G., Mullender, T.A.T., 2008. The rotation of Iberia during the Aptian and the opening of the Bay of Biscay. Earth Planet. Sci. Lett. 273 (1–2), 80–93.

Granado, P., Urgeles, R., Sàbat, F., Albert-Villanueva, E., Roca, E., Muñoz, J.A., Mazzuca, N., Gambini, R., 2016. Geodynamical framework and hydrocarbon plays of a salt giant: the NW Mediterranean Basin. Pet. Geosci. 22, 309–321.
Guimerà, J., 1984. Paleogene evolution of deformation in the northeastern Iberian Peninsula. Geol. Mag. 121, 413–420.
Guimerà, J., 2004. La Cadena Costera Catalana. In: Vera, J.A. (Ed.), Geología de España. SGE-IGME, Madrid, pp. 603–605.
Guimerà, 2018. Structure of an intraplate fold-and-thrust belt: the Iberian Chain. A synthesis. Geol. Acta 16 (4), 427–438.
Guimerà, J., Álvaro, M., 1990. Structure et évolution de la compression alpine dans la Chaîne ibérique et la Chaîne côtière catalane (Espagne). Bull. Soc. Géol. Fr. 6 (2), 339–348.
Guimerà, J., Santanach, P., 1978. Sobre la compresión alpina en el sector central de las Cadenas Costeras Catalanas. Acta Geol. Hisp. 2 (13), 33–42.
Guimerà, J., Alonso, A., Mas, J.R., 1995. Inversion of an extensional-ramp basin by a newly formed thrust: the Cameros basin (N. Spain). In: Buchanan, J.G., Buchanan, P. G. (Eds.), Basin Inversion, 88. Geological Society Special Publication, pp. 433–453.
Hansen, T.H., Clausen, O.R., Andresen, K.J., 2021. Thick- and thin-skinned basin inversion in the Danish Central Graben, North Sea – the role of deep evaporites and basement kinematics. Solid Earth 12, 1719–1747.
Hausegger, S., Kurz, W., Rabitsch, R., Kiechl, E., Brosch, F.J., 2010. Analysis of the internal structure of a carbonate damage zone: Implications for the mechanisms of fault breccia formation and fluid flow. J. Struct. Geol. 32 (9), 1349–1362.
Herraiz, M., De Vicente, G., Lindo-Naupari, R., Giner, J., Simon, J.L., Gonzalez-Casado, J. M., Vadillo, O., Rodriguez-Pascua, M.A., Cicuendez, J.I., Casas, A., Cabanas, L., Rincon, P., Cortes, A.L., Ramirez, M., Lucini, M., 2000. The recent (upper Miocene to Quaternary) and present tectonic stress distributions in the Iberian Peninsula. Tectonics 19, 762–786.
Hooker, J.N., Gomez, L.A., Laubach, S.E., Gale, J.F.W., Marrett, R., 2012. Effects of diagenesis (cement precipitation) during fracture opening on fracture aperture-size scaling in carbonate rocks. Geol. Soc. Lond., Spec. Publ. 370, 187–206.
Horváth, F., Berckhemer, H., 1982. Mediterranean backarc basins. In: Berckhemer, H., Hsü, K. (Eds.), Alpine Mediterranean Geodynamics. American Geophysical Union, Geodynamic Series A, 7, pp. 141–173.
Jackson, J.A., 1980. Reactivation of basement faults and crustal shortening in orogenic belts. Nature 283, 343–346.
Jones, M.A., Heller, P.L., Roca, E., Garcés, M., Cabrera, L., 2004. Time lag of syntectonic sedimentation across an alluvial basin: theory and example from the Ebro Basin, Spain. Basin Res. 16, 467–488.
Juez-Larré, J., 2003. Post Late Paleozoic Tectonothermal Evolution of the Northeast Margin of Iberia, Assessed by Fission-Track and (U-Th)/He Analysis, Ph.D. Thesis. Vrije Univ, Amsterdam.
Juez-Larré, J., Andriessen, P.A.M., 2006. Tectonothermal evolution of the northeastern margin of Iberia since the break-up of Pangea to present, revealed by low-temperature fission-track and (U–Th)/He thermochronology A case history of the Catalan Coastal Ranges. Earth Planet. Sci. Lett. 243, 159–180.
Julià, R., Santanach, P., 1984. Estructuras en la salbanda de falla paleógena de la falla del Vallès-Penedès (Cadenas Costeras Catalanas): su relación con el deslizamiento de la falla. Primer Congreso Español de Geología 1, 47–59.
Julià, R., Santanach, P., 1998. Banded structures in Gouge. In: Snoke, A.W., Tullis, J., Todd, V.R. (Eds.), Fault-Related Rocks: A Photographic Atlas. Princeton University Press, Princeton, pp. 56–57.
Lanaja, J.M., 1987. Contribución de la explotación petrolífera al conocimiento de la geología de España. IGME, Madrid.
Laubach, S.E., Eichhubl, P., Hargrove, P., Ellis, M.A., Hooker, J.N., 2014. Fault core and damage zone fracture attributes vary along strike owing to interaction of fracture growth, quartz accumulation, and differing sandstone composition. J. Struct. Geol. 68A, 207–226.
Lescoutre, R., Manatschal, G., 2020. Role of rift-inheritance and segmentation for orogenic evolution: example from the Pyrenean-Cantabrian System. BSGF-Earth Sci. Bull. 191, 18.
Li, Y.G., Vidale, J.E., Day, S.M., Oglesby, D.D., Cochran, E., 2003. Postseismic fault healing on the rupture zone of the 1999 M 7.1 Hector Mine, California, earthquake. Bull. Seismol. Soc. Am. 93, 854–869.
Llopis-Lladó, N., 1947. Contribución al conocimiento de la morfoestructura de los Catalánides. In: Inst. "Lucas Madalla". CSIC, Barcelona, p. 373.
López-Blanco, M., 2002. Sedimentary response to thrusting and fold growing on the SE margin of the Ebro Basin (Paleogene, NE Spain). Sediment. Geol. 146, 133–154.
López-Blanco, M., Marzo, M., Burbank, D.W., Vergés, J., Roca, E., Anadón, P., Piña, J., 2000. Tectonic and climatic controls on the development of foreland fan deltas: Montserrat and Sant Llorenç del Munt systems (Middle Eocene, Ebro Basin, NE Spain). Sediment. Geol. 138, 17–39.
Marcén, M., Casas-Sainz, A.M., Román-Berdiel, T., Griera, A., Santanach, P., Pocoví, A., Gil-Imaz, A., Aldega, L., Izquierdo-Llavall, E., 2018. Multiple movements recorded in a crustal weakness zone in NE Iberia: the Vallès-Penedès Fault revisited. J. Geodyn. 121, 96–114.
Marín, M., Roca, E., Marcuello, A., Cabrera, L., Ferrer, O., 2021. Mesozoic structural inheritance in the Cenozoic evolution of the central Catalan coastal ranges (western Mediterranean): structural and magnetotelluric analysis in the Gaià-Montmell high. Tectonophysics 814, 228970.
Martinell, J., 1988. An overview of the marine Pliocene of N.E. Spain. Géol. Méditerr. 15, 227–233.
Mencos, J., Carrera, N., Muñoz, J.A., 2015. Influence of rift basin geometry on the subsequent postrift sedimentation and basin inversion: the Organyà Basin and the Bóixols thrust sheet (south Central Pyrenees). Tectonics 34, 1452–1474.
Mercedes-Martín, R., Buatois, L.A., 2020. Microbialites and trace fossils from a Middle Triassic restricted carbonate ramp in the Catalan Basin, Spain: evaluating environmental and evolutionary controls in an epicontinental setting. Lethaia 54 (1), 4–25.
Micarelli, L., Benedicto, A., 2008. Normal fault terminations in limestones from the SE-Basin, France: implications for fluid flow. In: Wibberley, C.A.J., Kurtz, W., Imber, J., Holdsworth, R.E., Collettini, C. (Eds.), The Internal Structure of Fault Zones: Implications for Mechanical and Fluid-Flow Properties. Geological Society, 299. Special Publications, London, pp. 123–138.
Micklethwaite, S., Cox, S.F., 2004. Fault-segment rupture, aftershock-zone fluid flow and mineralization. Geol. Soc. Am. 32 (9), 813–816.
Moragas, M., Martínez, C., Baqués, V., Playà, E., Travé, A., Alías, G., Cantarero, I., 2013. Diagenetic evolution of a fractured evaporite deposit (Vilobí Gypsum Unit, Miocene, NE Spain). Geofluids 13 (2), 180–193.
Muñoz, J.A., 1992. Evolution of a continental collision belt: ECORS-Pyrenees crustal balanced cross-section. In: McClay, K. (Ed.), Thrust Tectonics. Chapman & Hall, London, pp. 235–246.
Muñoz, J.A., 2017. Fault-related folds in the southern Pyrenees. AAPG Bull. 101-4, 579–587.
Naccio, D.Di., Boncio, P., Cirilli, S., Casaglia, F., Morettini, E., Laveccnia, G., Brozzetti, F., 2005. Role of mechanical stratigraphy on fracture development in carbonate reservoirs: insights from outcropping shallow wáter carbonates in the Umbria-Marche Apennines, Italy. J. Volcanol. Geotherm. Res. 148, 98–115.
Nebot, M., Guimerà, J., 2016. Structure of an inverted basin from subsurface and field data: the late Jurassic-early cretaceous Maestrat Basin (Iberian Chain). Geol. Acta 14 (2), 155–177.
Ortí, F., Pérez-López, A., Salvany, J.M., 2017. Triassic evaporites of Iberia: sedimentological and palaeogeographical implications for the western Neotethys evolution during the Middle Triassic–Earliest Jurassic. Palaeogeogr. Palaeoclimatol. Palaeoecol. 471, 157–180.
Ortiz, G., Stevens Goddard, A.L., Fosdick, J.C., Alvarado, P., Carrapa, B., Cristofolini, E., 2021. Fault reactivation in the Sierras Pampeanas resolved across Andean extensional and compressional regimes using thermochronologic modeling. J. S. Am. Earth Sci. 112, 103533.
Parcerisa, D., 2002. Petrologia i diagènesi en sediments de l'Oligocè superior i del Miocè inferior i mitjà de la Depressió del Vallès i del Pla de Barcelona. Evolució de l'àrea Font i dinámica dels fluids. Dissertation. Universitat Autònoma de Barcelona, p. 261.
Parcerisa, D., Gómez-Gras, D., Travé, A., 2005. A model of early calcite cementation in alluvial fans: evidence from the Burdigalian sandstones and limestones of the Vallès-Penedès half-graben (NE Spain). Sediment. Geol. 178, 197–217.
Peacock, D., Tavarnelli, E., Andreson, M., 2016. Interplay between stress permutations and overpressure to cause strike-slip faulting during tectonic inversion. Terra Nova 29-1, 61–70.
Perez, N., Horton, B., Carlotto, V., 2016. Structural inheritance and selective reactivation in the Central Andes: Cenozoic deformation guided by pre-Andean structures in southern Peru. Tectonophysics 671, 264–280.
Robles, S., 1982. El Cretácico de los Catalánides. In: El Cretácico de España. Universidad Complutense de Madrid, Madrid, pp. 199–272.
Roca, E., 1994. La evolución geodinámica de la Cuenca Catalano-Balear y áreas adyacentes desde el Mesozoico hasta la actualidad. Acta Geol. Hisp. 29 (1), 3–25.
Roca, E., 2001. The Northwest-Mediterranean basin (Valencia Trough, Gulf of Lions and Liguro-Provencal basins): structure and geodynamic evolution. In: Ziegler, P.A., Cavazza, W., Robertson, A.H.F., Crasquin-Soleau, S. (Eds.), Peri-Tethys Memoir 6: Peri-Tethyan Rift/Wrench Basins and Passive Margins. French National Museum of Natural History, 186, pp. 671–706.
Roca, E., Guimerà, J., 1992. The Neogene structure of the eastern Iberian margin: structural constraints on crustal evolution of the Valencia Trough (western Mediterranean). Tectonophysics 203, 203–218.
Roca, E., Sans, M., Cabrera, Ll, Marzo, M., 1999. Oligocene to middle Miocene evolution of the central Catalan margin (northwestern Mediterranean). Tectonophysics 315, 209–233.
Transect II: Aquitaine Basin - Pyrenees - Ebro Basin - Catalan Range - Valencia Trough - Balearic Block - Algerian Basin - Kabylies - Atlas - Saharan Platform. In: Roca, E., Frizon de Lamotte, D., Mauffret, A., Bracène, R., Vergés, J., Benaouali, N., Fernández, M., Muñoz, J.A., Zeyen, H., Cavazza, W., Roure, F.M., Spakman, W., Stampfli, G.M., Ziegler, P.A. (Eds.), 2004. 2004. The Transmed Atlas – The Mediterranean Region from Crust to Mantle. Springer, Berlin, Heidelberg.
Roma, M., Ferrer, O., Roca, E., Pla, O., Escosa, F.O., Butillé, M., 2018. Formation and inversion of salt-detached ramp-syncline basins. Results from T analog modeling and application to the Columbrets Basin (Western Mediterranean). Tectonophysics 745, 214–228.
Romagny, A., Jolivet, L., Menant, A., Bessière, E., Maillard, A., Canva, A., Gorini, Ch., Augier, R., 2020. Detailed tectonic reconstructions of the Western Mediterranean region for the last 35 Ma, insights on driving mechanisms. BSGF - Earth Sci. Bull. 191 (37), 45.
Rosenbaum, G., Lister, G.S., Duboz, C., 2002. Relative motions of Africa, Iberia, and Europe during Alpine orogeny. Tectonophysics 359, 117–129.
Sàbat, F., Roca, E., Muñoz, J.A., Vergés, J., Santanach, P., Sans, M., Masana, E., Estévez, A., Santisteban, C., 1997. Role of extension and compression in the evolution of eastern margin of Iberia: the ESCI-Valencia Trough seismic profile. Rev. Soc. Geol. Esp. 8 (4), 431–448.
Salas, R., 1987. El Malm i el Cretaci inferior entre el Massís de Garraf i la Serra d'Espadà. Ph.D. Thesis. Universitat de Barcelona, p. 345.
Salas, R., Casas, A., 1993. Mesozoic extensional tectonics, stratigraphy, and crustal evolution during the Alpine cycle of the eastern Iberian basin. Tectonophysics 228 (1–2), 33–55.

Salas, R., Guimerà, J., Mas, R., Martín-Closas, C., Meléndez, A., Alonso, A., 2001. Evolution of the Mesozoic Central Iberian Rift system and its Cainozoic inversion (Iberian Chain). In: Ziegler, P.A., Cavazza, W., Robertson, A.H.F., Crasquin-Soleau, S. (Eds.), Peri-Tethys Memoir 6: Peri-Tethyan Rift/Wrench Basins and Passive Margins. French National Museum of Natural History, 186, pp. 145–185.

Salas, R., Guimerà, J., Bover-Arnal, T., Nebot, M., 2020. The Iberian-Catalan linkage: the Maestrat and Garraf Basin. In: Quesada, Oliveira (Eds.), The Geology of Iberia: A geodynamic approach. Regional geology reviews Vol. 3, Ch. 5, pp. 228–230.

Santanach, P., Casas, J.M., Gratacós, O., Liesa, M., Muñoz, J.A., Sàbat, F., 2011. Variscan and Alpine structure of the hills of Barcelona: geology in an urban area. J. Iber. Geol. 37 (2), 121–136.

Scisciani, V., Patruno, S., D'Intino, N., Esestime, P., 2022. Paleozoic basin reactivation and inversion of the underexplored Northern North Sea platforms: a cross-border approach. Geol. Soc. Lond., Spec. Publ. 494, 301–331.

Serra, P.R., Enrique, P., 1989. The Late-Hercynian intrusives from southern Catalonian Coastal Ranges (NE Spain), and their epiplutonic to subvolcanic level of magma emplacement. Rend. Soc. Ital. Mineral. Petrol. 43, 817–829.

Sibson, R., 2003. Brittle-failure controls on maximum sustainable overpressure in different tectonic regimes. AAPG Bull. 87-6, 901–908.

Sibuet, J.C., Srivastava, S., Spakman, W., 2004. Pyrenean orogeny and plate kinematics. J. Geophys. Res. 109, B08104.

Soliva, R., Benedicto, A., Vergély, P., Rives, T., 2005a. Mechanical control of a lithological alternation on normal fault morphology, growth and reactivation. Bull. Soc. Géol. Fr. 176 (4), 329–342.

Soliva, R., Schultz, R., Benedicto, A., 2005b. Three-dimensional displacement-length scaling and maximum fault length in layered rocks. Geophys. Res. Lett. 32, L16302.

Soliva, R., Benedicto, A., Maerten, L., 2006. Spacing and linkage of confined normal faults: importance of mechanical thickness. J. Geophys. Res. 111, B01402.

Srivastava, S.P., Roest, W.R., Kovacs, L.C., Oakey, G., Lévesque, S., Verhoef, J., Macnab, R., 1990. Motion of Iberia since the late Jurassic: results from detailed aeromagnetic measurements in the Newfoundland Basin. Tectonophysics 184, 229–260.

Teixell, A., Arboleya, M.L., Julivert, M., 2003. Tectonic shortening and topography in the central High Atlas (Morocco). Tectonics 22 (5), 1051.

Torabi, A., Johannessen, M.U., Ellingsen, T.S.S., 2019. Fault core thickness: insights from Silicilastic and Carbonate rocks. Geofluids 2019, 24 article ID 2918673.

Travé, A., Calvet, F., 2001. Syn-rift geofluids in fractures related to the early-middle Miocene evolution of the Vallès-Penedès half-graben (NE Spain). Tectonophysics 336 (1–4), 101–120.

Travé, A., Calvet, F., Soler, A., Labaume, P., 1998. Fracturing and fluid migration during Paleogene compression and Neogene extension in the Catalan Coastal Ranges, Spain. Sedimentology 45, 1063–1082.

Travé, A., Roca, E., Playà, E., Parcerisa, D., Gómez-Gras, D., 2009. Migration of Mn-rich fluids through normal faults and fine-grained terrigenous sediments during early development of the Neogene Vallès-Penedès half-graben (NE Spain). Geofluids 9, 303–320.

Travé, A., Rodríguez-Morillas, N., Baqués, V., Playà, E., Casas, L., Cantarero, I., Martín-Martín, J.D., Gómez-Rivas, E., Moragas, M., Cruset, D., 2021. Origin of the coloured karst fills in the Neogene extensional system of NE Iberia (Spain). Minerals 2021 (11), 1382.

Underwood, C.A., Cooke, M.L., Simo, J.A., Muldon, M.A., 2003. Stratigraphic controls on vertical fracture patterns in Silurian dolomite, northeastern Wisconsin. AAPG Bull. 87 (1), 121–142.

Van Hinsbergen, D.J.J., Vissers, R.L.M., Spakman, W., 2014. Origin and consequences of western Mediterranean subduction, rollback, and slab segmentation. Tectonics 33, 393–419.

Van Hinsbergen, D.J.J., Torsvik, T.H., Schmid, S.M., Matenco, L.C., Maffione, M., Vissers, R.L.M., Gürer, D., Spakman, W., 2020. Orogenic architecture of the Mediterranean region and kinematic reconstruction of its tectonic evolution since the Triassic. Gondwana Res. 81, 79–229.

Vaquer, R., 1973. El metamorfismo y las rocas plutónicas y filonianas de la Sierra de Collcerola (Tibidabo), Barcelona. Doctoral Thesis. Universitat de Barcelona, p. 362.

Vergés, J., Fernàndez, M., Martínez, A., 2002. The Pyrenean origin: pre-, syn-, and post-collisional evolution. In: Rosenbaum, G., Lister, G.S. (Eds.), 2002. Reconstruction of the Evolution of the Alpine-Himalayan orogen. Journal of the Virtual Explorer, 8, pp. 57–76.

Vergés, J., Moragas, M., Martín-Martín, J.D., Saura, E., Razin, P., Grelaud, C., Malaval, M., Joussiaume, R., Messager, G., Sharp, I., Hunt, D.W., 2017. Salt tectonics in the Atlas Mountains of Morocco. In: Soto, J.I., Tari, G., Flinch, J. (Eds.), Permo-Triassic Salt Provinces of Europe, North Africa and the Atlantic Margins. Tectonics and hydrocarbon potential. Elsevier, Amsterdam, the Netherlands, pp. 563–576, 2017.

Vidal, N., Gallart, J., Dañobeitia, J., Díaz, J., 1995. Mapping the Moho in the Iberian Mediterranean margin by multicoverage processing and merging of wide-angle and near-vertical reflection data. In: Banda, E., Torné, M., Talwani, M. (Eds.), Rifted Ocean Continent Boundaries. NATO ASI Series C, Mathematical and Physical Sciences, 463, pp. 291–308.

Vidal, N., Gallart, J., Dañobeitia, J.J., 1998. A deep seismic crustal transect from the NE Iberian Peninsula to the western Mediterranean. J. Geophys. Res. 103, 12381–12396.

Virgili, C., 1958. El Triásico de los Catalánides. Bol. Inst. Geol. Min. Esp. 69, 856.

Wang, C.Y., Mao, N., Wu, F.T., 1980. Mechanical properties of clays at high pressure. J. Geophys. Res. 85, 1462–1468.

Wintsch, R., Christoffersen, R., Kronenberg, A., 1995. Fluid-rock reaction weakening of fault zones. J. Geophys. Res. 100, 13021–13032.

Zwaan, F., Schreurs, G., Buiter, S., Ferrer, O., Reitano, R., Rudolf, M., Willingshofer, E., 2022. Analogue modelling of basin inversion: a review and future perspectives. In: Solid Earth Discuss. [Preprint]. https://doi.org/10.5194/se-2022-8 in review.